View metadata, citation and similar papers at core.ac.uk

brought to you by CORE

provided by INRIA a CCSD electronic archive server

Analysis of the Competition between Wired, DSL and Wireless TCP Flows in an Access Network

François Baccelli, Ki Baek Kim, Danny de Vleeschauwer

To cite this version:

François Baccelli, Ki Baek Kim, Danny de Vleeschauwer. Analysis of the Competition between Wired, DSL and Wireless TCP Flows in an Access Network. [Research Report] RR-5306, INRIA. 2004, pp.39. inria-00070694

HAL Id: inria-00070694

https://hal.inria.fr/inria-00070694

Submitted on 19 May 2006

HAL is a multi-disciplinary open access archive for the deposit and dissemination of scientific research documents, whether they are published or not. The documents may come from teaching and research institutions in France or abroad, or from public or private research centers.

L'archive ouverte pluridisciplinaire **HAL**, est destinée au dépôt et à la diffusion de documents scientifiques de niveau recherche, publiés ou non, émanant des établissements d'enseignement et de recherche français ou étrangers, des laboratoires publics ou privés.

INSTITUT NATIONAL DE RECHERCHE EN INFORMATIQUE ET EN AUTOMATIQUE

Analysis of the Competition between Wired, DSL and Wireless TCP Flows in an Access Network

François Baccelli — Ki Baek Kim — Danny De Vleeschauwer

N° 5306

Septembre 2004

THÈME 1

ISSN 0249-6399 ISRN INRIA/RR--5306--FR+ENG

Analysis of the Competition between Wired, DSL and Wireless TCP Flows in an Access Network

François Baccelli* , Ki Baek Kim† , Danny De Vleeschauwer‡

Thème 1 —Réseaux et systèmes
Projet TREC

Rapport de recherche n° 5306 —Septembre 2004 —39 pages

Abstract: This paper analyzes the performance of a large population composed of several classes of long lived TCP flows experiencing packet losses due to random transmission errors and to congestion created by the sharing of a common tail-drop or AQM bottleneck router. Each class has a different transmission error rate. This setting is used to analyze the competition between wired and wireless users in an access network, where one class (the wired class) has no or small (like BER in DSL) transmission error losses whereas the other class has higher transmission error losses, or the competition between DSL flows using different coding schemes. We propose a natural and simple model for the joint throughput evolution of several classes of TCP flows under such a mix of losses. Two types of random transmission error losses are considered: one where losses are Poisson and independent of the rate of the flow, and one where the losses are still Poisson but with an intensity that is proportional to the rate of the source. We show that the large population model where the population tends to infinity has a threshold on the transmission error rate (given in closed form) above which there are no congestion losses at all in steady state, and below which the stationary state is a periodic congestion regime in which we compute both the mean value and the distribution of the rate obtained by each class of flow. We also show that the maximum mean value for the aggregated rate is achieved at the threshold. For the finite population model and models based on other classes of point processes, a sufficient condition is obtained for the existence of congestion times in the case of arbitrary transmission error point processes.

Key-words: TCP, congestion control, flow control, AIMD, IP traffic, synchronization, throughput, wireless, DSL, bit error, packet error, transmission error, mean field, Mellin transform.

* INRIA-ENS, 45 rue d'Ulm 75005, Paris, France, francois.baccelli@ens.fr
† INRIA-ENS, 45 rue d'Ulm 75005, Paris, France, kkb@di.ens.fr
‡ ALCATEL-NSG, Fr. Wellesplein 1, B-2018 Antwerp, Belgium, Danny.De_Vleeschauwer@alcatel.be

Unité de recherche INRIA Rocquencourt
Domaine de Voluceau, Rocquencourt, BP 105, 78153 Le Chesnay Cedex (France)
Téléphone : +33 1 39 63 55 11 —Télécopie : +33 1 39 63 53 30

Analyse de la concurrence entre des flots TCP filaires, DSL et sans fils sur un réseau d'accès

Résumé : Nous étudions dans cet article les performances d'une population formée d'un grand nombre de flots TCP persistants qui se répartissent en plusieurs classes subissant des pertes de paquets aléatoires de deux types: des pertes dues à des erreurs de transmission et des pertes dues à la congestion résultant du partage par ces flots d'un routeur commun. Chaque classe a son taux d'erreur de transmission. Ce cadre permet de considérer les situations suivantes: la concurrence entre des flots filaires et sans fils sur un réseau d'accès, où la classe filaire ne subit aucune perte de transmission de paquet ou de petites pertes (comme le *Bit Error Rate* (BER) des flots DSL), tandis que la classe sans fils subit des pertes de transmission plus fréquentes; la concurrence entre deux types de flots DSL utilisant des codages différents. Nous proposons un modèle simple et assez naturel pour l'évolution jointe des débits de ces diverses classes de flots TCP. Nous considérons deux modèles pour les erreurs de transmission: des pertes suivant des lois de Poisson à taux constant et donc indépendant du débit des flots et des pertes suivant des lois de Poisson avec une intensité proportionnelle au débit du flot. Nous étudions le modèle où la taille de la population tend vers l'infini. Nous montrons qu'il existe un seuil positif sur les pertes de transmission (donné explicitement) au dessus duquel il n'y a pas de pertes de congestion et en dessous duquel l'état stationnaire est un régime avec des congestions périodiques, dans lequel nous pouvons calculer la moyenne et la distribution du débit de chaque flot. Nous montrons aussi que le débit agrégé optimal est obtenu au seuil. Le modèle avec population finie et ceux fondés sur d'autres classes de processus ponctuels sont aussi étudiés. En particulier, nous donnons une condition suffisante d'existence de pertes par congestion valable pour tout modèle, indépendamment de la taille de la population et du type des processus ponctuels des pertes par erreur de transmission.

Mots-clés : TCP, contrôle de congestion, contrôle de flux, algorithme de croissance additive et décroissance multiplicative, trafic IP, synchronisation, débit, sans fil, DSL, erreur par bit, erreur par paquet, erreur de transmission, champ moyen, transformée de Mellin.

1 Introduction

Understanding the behavior of TCP (Transmission Control Protocol) in the presence of random transmission packet losses has become important with the current increase of the proportion of wireless and of DSL (Digital Subscriber Line) users in the Internet [10], for which bit/packet error rates are essential features. Since random transmission losses may be mistakenly considered as congestion information by congestion control mechanisms based on losses, such a protocol will not work as expected.

The present paper studies the interaction of several classes of TCP flows with different transmission error rates and different RTTs (Round Trip Time) which may experience congestion losses in a common access link. This setting allows us to analyze the dynamic behavior of mixed wired and wireless users, and the performance of the competition of DSL links with different coding schemes: *Fast* with a small RTT but a large bit (and hence packet) error rate and *Interleaved* with a large RTT but a small bit error rate [1].

Previous studies on TCP over hybrid wired/wireless links have primarily focused on improving the performance by adding some mechanisms, which are used to either hide or reduce the wrong congestion information [2, 3, 4]. [5] proposed an explicit throughput formula for homogeneous flows subject to both congestion and transmission losses. Two interesting and non-intuitive properties were reported:

1. there exists a positive threshold (given in closed form) on the transmission error rate above which there are no congestion losses at all in steady state;

2. below this threshold, the mean throughput of each flow is an increasing function of the transmission error rate, so that the maximum mean value is in fact achieved when the transmission error rate is equal to this threshold.

However, [5] only considered the case where all users have the same rate-independent Poisson transmission error rate and the same RTT, and concentrated on mean value analysis.

The present paper proposes a more general framework which allows one to evaluate the mean throughput in e.g. the rate-independent, the rate-dependent and the mixed rate-independent/dependent error cases, and in multiclass cases with different error rates and RTTs. It also provides new results on the stationary distribution of the rate obtained by each class. The knowledge of distributions allows one to predict the proportion of time that a given flow has a rate above a predefined value, which is of practical interest for assessing quality of service and possibly proposing SLAs (Service Level Agreement) within this context.

In §2, we introduce the problem setting and describe the large population model, which is used in most of the paper, and its two limiting regimes: the congestionless regime and the congestion regime.

In §3, we derive partial differential equations for the distributions of the rates of the congestionless regime. We study both of the rate-independent and the rate-dependent transmission error cases, and then the mixed error case. We give closed form solutions for the stationary distributions.

In §4, we use the dynamic equations of the congestionless regime, to derive the mean values and the distributions of the throughput in the stationary congestion regime. We give simple conditions

guaranteeing the existence of the congestion regime. We prove that in the rate-independent tail-drop case, the congestion regime has a unique periodic limiting regime. We also show that in this case, the maximum mean value of the aggregated throughput is achieved at the threshold. In the rate-dependent and mixed cases, the mean values and the distributions of the congestion regime are calculated numerically. For the finite population model and models based on other classes of point processes, a sufficient condition is obtained for the existence of congestion times in the case of arbitrary transmission error point processes.

In §5, we report on the three main solution methods used to solve the equations of §3 and 4: *Maple* for closed form solutions involving e.g. infinite products; *Mathcad* for the numerical solution of the linear integral equations; finally *Netscale* [6] for simulating these large population TCP models.

Section 6 contains two case studies based on the methodology developed in the paper: the competition between TCP users using two coding modes called *Interleaved* and *Fast* in a DSL access network; the competition between wired and wireless TCP users in an access network.

Finally, Section 7 gathers a few results on the finite population model.

2 Interaction of Heterogeneous TCP Flows Sharing an Access Link

2.1 Interaction Model

The setting consists of M classes of persistent TCP controlled users competing for the bandwidth of one access link or router. Some classes have a wireless connection, others a wired one, possibly via a DSL end-link. All these classes hence differ in their RTT and their bit error processes.

Some wired users in an access network have 0 BER (Bit Error Rate); others like e.g. those using DSL lines have a moderate BER that may depend on the coding scheme they use. Wireless users (for instance WIFI (Wireless Fidelity) users accessing the network via a DSL link) are often prone to higher BER. Bit error processes may have different statistical properties for different classes. For instance, some DSL end-links are prone to impulse errors that take place at random times and independently of the rate of the flow [7], a situation that will be referred to as the RI (Rate-Independent) case throughout the paper, whereas most wireless and DSL connections would be subject to some BER that leads to packet losses with an intensity that depends on the instantaneous rate of the flow (RD (Rate-Dependent) case). In addition, transmission error losses in some wireless cases may have a complex correlation structure like in e.g. Gilbert's Markovian model [8, 9]. In the present paper, we will focus on the case without correlation structure which seems to be natural for the DSL case and leave the study of the more complex case like Gilbert's loss model to a future paper.

We will denote by R_m the RTT for class m. The RTT may vary from one class to another depending on the propagation delay between the source and the destination of the TCP connections; for instance, a first subpopulation in a DSL access network may download data from a close cache and hence have a small common RTT, whereas the other users may be arranged in a few homogeneous classes depending on the propagation delay between source and destination. Another cause of RTT variability is the coding scheme that is chosen by users when applicable (e.g. DSL or wireless

users). In this paper, we will mainly focus on the case with small buffers where the RTT of a given user can be considered constant over time.

On top of these transmission error losses come congestion losses that stem from loss/discard in the buffer of the shared link. Two cases will be considered: RED (Random Early Detection) and tail-drop.

We assume that a TCP Reno-like control protocol is used where all flows are in the congestion avoidance phase, so that the window of any given flow has

- a linear increase of α_m (for instance equal to $\frac{1}{R_m}$) per second at any given time; the rate of a flow and the window size are linked by a Little like law, so that the linear increase of the window leads to a linear increase of the rate, with slope $\frac{\alpha_m}{R_m}$.
- a multiplicative decrease which consists of a division of the rate by 2 at any negative signal experienced by the flow, whatever its nature (transmission loss, marking in the RED buffer or loss due to overflow of the tail-drop buffer).

An important feature of the competition concerns the synchronization of flows. Transmission errors and RED marking decisions lead to unsynchronized losses that affect one flow at a time, whereas buffer overflows that may happen both in the RED and tail-drop policies may lead to partially or even fully synchronized losses where many flows halve their rate almost simultaneously. The parameter p (referred to as the synchronization rate) describes the proportion of flows that simultaneously experience a loss during a congestion epoch. For queueing theory estimates of this parameter, see [11].

The main difficulty with this class of models stems from the following examples of logical loops:

- the frequency at which bits or packets are lost due to rate dependent transmission losses depends (by definition) on the rate achieved by each source, which is precisely what we look for;
- the frequency at which buffer overflows occur depends on the instantaneous rates of the flows, which again is what we look for.

An example of interaction process with two flows and full synchronization is depicted in Figure 1.

The aim of this paper is to provide an analytic model allowing one to predict the mean values and the fluctuations of the rate obtained by each class.

2.2 The Large Population Model

We denote by N_m the number of TCP flows of class m, which we assume to be constant over time; let $N = \sum N_m$ and $r_m = \frac{N_m}{N}$, then we have $\sum r_m = 1$.

We assume that the capacity of the bottleneck router is $C = c \times N$.

Let $X^{i,m}(t)$ denote the throughput of flow i of class m at time t for the system of parameter N. Then the aggregated throughput of class m at time t can be defined as

$$X^m(t) \quad = \quad \frac{1}{N_m} \sum_{i=1}^{N_m} X^{i,m}(t).$$

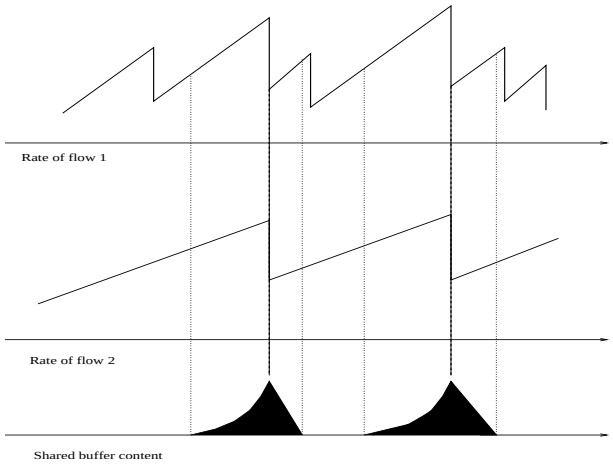

Figure 1: Example of two competing TCP classes sharing a tail-drop link. Class 1 has a short RTT but is transmission error prone, whereas class 2 has a longer RTT but no transmission errors.

The case obtained when letting N go to ∞ in the last model is referred to as the large population model. This model will be used throughout the paper except in § 7. Using techniques similar to those in [5], it can be shown that for all m and t, the random variable $X^m(t)$ converges almost surely to a deterministic limit $\overline{X}^m(t)$ that we describe and analyze in the next section. We define the large population aggregated throughput as

$$\overline{X}(t) \equiv \lim_{N\to\infty} \frac{1}{N} \sum_m \sum_i X^{i,m}(t).$$

Then for all t,

$$\overline{X}(t) = \sum_m r_m \overline{X}^m(t). \quad (1)$$

2.3 The Two Large Population Regimes

As we shall see below, and as already observed in the homogeneous (or single class) model case [5], the large population limit has at least two stationary regimes, i.e., the congestionless and the congestion regimes.

In the congestionless regime, the buffer never fills in as transmission error losses throttle the rate of the flows in such a way that in the large population model, the sum of the stationary rates is not sufficient to reach the link capacity.

In the congestion regime, the regulation stems from both transmission error losses and congestion losses or marking. In the AQM (Active Queue Management) case, one possible stationary regime

is that where the buffer stabilizes to a fixed value which in turn leads to a constant packet marking probability [12, 13]. In the tail-drop case, we will limit ourselves to the small buffer case where a possible stationary congestion regime consists of a periodic buffer overflow, and hence, synchronized or partially synchronized losses for the flows.

3 Congestionless Regimes

In the large population regime, let $s_m(z,t)$ denote the density of flows of class m that have a rate of $z \in \mathbb{R}^+$ at time $t \in \mathbb{R}^+$. In this section, we focus on the case when $c = \infty$, so that congestion never takes place.

3.1 The RI Transmission Error Case

Using techniques similar to those of [14], for the case where the transmission error intensity of a flow of class m is constant with λ_m, one obtains that these functions satisfy the (free process) partial differential equation (PDE)

$$\frac{\partial s_m}{\partial t}(z,t) \; + \; \frac{\alpha_m}{R_m}\frac{\partial s_m}{\partial z}(z,t) \quad = \quad \lambda_m(2s_m(2z,t) - s_m(z,t)). \tag{2}$$

When multiplying both sides of (2) by z and integrating w.r.t. z, it is easy to check that the mean value at each time t

$$\overline{X}^m(t) \quad = \quad \int_0^\infty z \; s_m(z,t) \; dz$$

satisfies the ODE

$$\frac{d\overline{X}^m(t)}{dt} \quad = \quad -\frac{\lambda_m}{2}\overline{X}^m(t) \; + \; \frac{\alpha_m}{R_m}.$$

This immediately gives

$$\overline{X}^m(t) \quad = \quad \left(\overline{X}^m(0) - \frac{\alpha_m}{R_m}\frac{2}{\lambda_m}\right) e^{-\frac{\lambda_m t}{2}} \; + \; \frac{\alpha_m}{R_m}\frac{2}{\lambda_m}. \tag{3}$$

Lemma 1 *The solution of this free process PDE is given by the following integral equation:*

$$\begin{aligned} s_m(z,t) \quad = \quad & s_m\left(z - t\frac{\alpha_m}{R_m}, 0\right) e^{-\lambda_m t} \\ & + \; 2\lambda_m \int_0^t e^{-\lambda_m u} s_m\left(2\left(z - u\frac{\alpha_m}{R_m}\right), t-u\right) du \end{aligned} \tag{4}$$

which is a Fredholm equation of the second kind in the unknown $s_m(z,t)$ if one considers $s_m(z,0)$ as a data.

The proof can be found in Appendix 9.1.

Equation (4) is easy to interpret when considering the two cases: for the rate to be z at time t, either there was no loss between time 0 and time t, which requires that the rate was $z - t\frac{\alpha_m}{R_m} \geq 0$ at time 0, or there was at least one loss; in this case, the last loss takes place at time $t-u$ with probability $e^{-\lambda_m u}\lambda_m du$ and the rate just before time $t-u$ should be $2\left(z - u\frac{\alpha_m}{R_m}\right)$.

The following lemma studies the steady state solution of the PDE (2).

Lemma 2 *The stationary solution of (2) is*

$$\sigma_m(z) \quad = \quad \phi \sum_{n\geq 0} a_n e^{-\left(\lambda_m \frac{R_m}{\alpha_m} 2^n\right) z} \tag{5}$$

with

$$\phi \quad = \quad \left(\frac{\alpha_m}{\lambda_m R_m} \prod_{k\geq 1} (1 - 2^{-k}) \right)^{-1}$$

and with a_n the coefficients of the expansion

$$\prod_{k\geq 0} (1 - 2^{-k} x) \quad = \quad \sum_{n\geq 0} a_n x^n.$$

Its mean is

$$\overline{v}_m \quad = \quad \frac{2\alpha_m}{\lambda_m R_m}. \tag{6}$$

The proof can be found in Appendix 9.2.

3.2 The RD Transmission Error Case

We now focus on the case where the transmission error intensity of a flow of class m with rate x is $\mu_m x$. The PDE associated with this case is

$$\frac{\partial s_m}{\partial t}(z,t) \; + \; \frac{\alpha_m}{R_m}\frac{\partial s_m}{\partial z}(z,t) \quad = \quad \mu_m(4z s_m(2z,t) \; - \; z s_m(z,t)). \tag{7}$$

By the same type of arguments as above, one gets:

Lemma 3 *The solution of the free process PDE (7) is again given by the Fredholm equation:*

$$\begin{aligned} s_m(z,t) \quad &= \quad s_m\left(z - t\frac{\alpha_m}{R_m}, 0\right) e^{-\mu_m\left(zt - \frac{\alpha_m t^2}{2R_m}\right)} \\ &+ \quad 4\mu_m \int_0^t e^{-\mu_m\left(zu - \frac{\alpha_m u^2}{2R_m}\right)} \left(z - u\frac{\alpha_m}{R_m}\right) s_m\left(2\left(z - u\frac{\alpha_m}{R_m}\right), t-u\right) du. \end{aligned} \tag{8}$$

The following lemma studies the steady state solution of the PDE (7).

Lemma 4 *The stationary solution of (7) is*

$$\sigma_m(z) \quad = \quad 2\phi \sum_{n\geq 0} a_n e^{-\left(\frac{\mu_m R_m}{2\alpha_m} 4^n\right) z^2} \tag{9}$$

with

$$\phi \quad = \quad \left(\sqrt{\pi} \left(\frac{2\alpha_m}{\mu_m R_m} \right)^{\frac{1}{2}} \prod_{k\geq 1} (1 - 2^{-2k+1}) \right)^{-1}$$

and with a_n the coefficients of the expansion

$$\prod_{k\geq 0} (1 - 2^{-2k} x) \quad = \quad \sum_{n\geq 0} a_n x^n.$$

Its mean is

$$\overline{v}_m \quad = \quad \sqrt{\frac{2\alpha_m}{\mu_m R_m}} \sqrt{\frac{1}{\pi}} \frac{\prod_{k\geq 1}(1 - 2^{-2k})}{\prod_{k\geq 1}(1 - 2^{-2k+1})}. \tag{10}$$

See Appendix 9.3 for the proof.

Figure 2, 3 and 4 illustrate (5), (9) and (10), respectively. All numerical results in this section are derived using *Maple*.

3.3 The Mixed RI-RD Transmission Error Case

The PDE of the mixed RI-RD error case with the transmission error density $\lambda_m + \mu_m x$ is

$$\begin{aligned} \frac{\partial s_m}{\partial t}(z,t) \; + \; \frac{\alpha_m}{R_m} \frac{\partial s_m}{\partial z}(z,t) \quad &= \quad \lambda_m (2 s_m(2z,t) \; - \; s_m(z,t)) \\ &\quad + \; \mu_m (4 z s_m(2z,t) \; - \; z s_m(z,t)). \end{aligned} \tag{11}$$

By the same type of arguments as above, one gets:

Lemma 5 *The solution of the free process PDE (11) is given by the Fredholm equation:*

$$\begin{aligned} s_m(z,t) \quad = \quad & s_m \left(z - t\frac{\alpha_m}{R_m}, 0 \right) e^{-\lambda_m t - \mu_m \left(zt - \frac{\alpha_m t^2}{2R_m} \right)} \\ & + \; \int_0^t e^{-\lambda_m u - \mu_m \left(zu - \frac{\alpha_m u^2}{2R_m} \right)} \left(2\lambda_m + 4\mu_m \left(z - u\frac{\alpha_m}{R_m} \right) \right) \\ & .s_m \left(2 \left(z - u\frac{\alpha_m}{R_m} \right), t - u \right) du. \end{aligned} \tag{12}$$

The proof can be found in Appendix 9.1.

In the next section, we focus on the case when c is finite which can lead to the congestion regime.

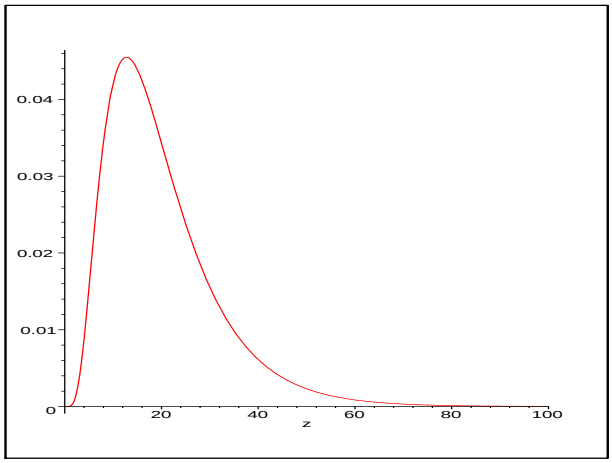

Figure 2: Stationary distribution (5) when $\lambda_m = 0.1$ 1/s, $R_m = \frac{1}{\alpha_m} = 1$ s.

4 The Structure of the Congestion Regime

4.1 The AQM Case

Here we concentrate on the AQM case with a constant packet drop probability at equilibrium point. Such a constant AQM packet drop probability takes place when assuming stabilization, namely convergence to a non-oscillatory regime.

Consider $N_m = r_m N$ statistically identical TCP controlled flows with RTT R_m and packet error rate μ_m.

The first possible large population regime is the congestionless regime where the packet transmission error rates alone stabilize the access network. In the case of rate dependent transmission errors, this is the case when

$$\sum_m r_m \sqrt{\frac{2\alpha_m}{\mu_m R_m}} \quad < \quad c\sqrt{\pi}\frac{\prod_{k\geq 1}(1-2^{-2k+1})}{\prod_{k\geq 1}(1-2^{-2k})} \tag{13}$$

in view of (10).

If this condition is not satisfied, then there ought to be a positive AQM packet drop probability, common to all flows which helps stabilizing the network. Using monotonicity arguments, it is easy to show that β is then the unique solution of the following equation:

$$\sum_m r_m \sqrt{\frac{2\alpha_m}{(\mu_m+\beta) R_m}} \quad = \quad c\sqrt{\pi}\frac{\prod_{k\geq 1}(1-2^{-2k+1})}{\prod_{k\geq 1}(1-2^{-2k})}. \tag{14}$$

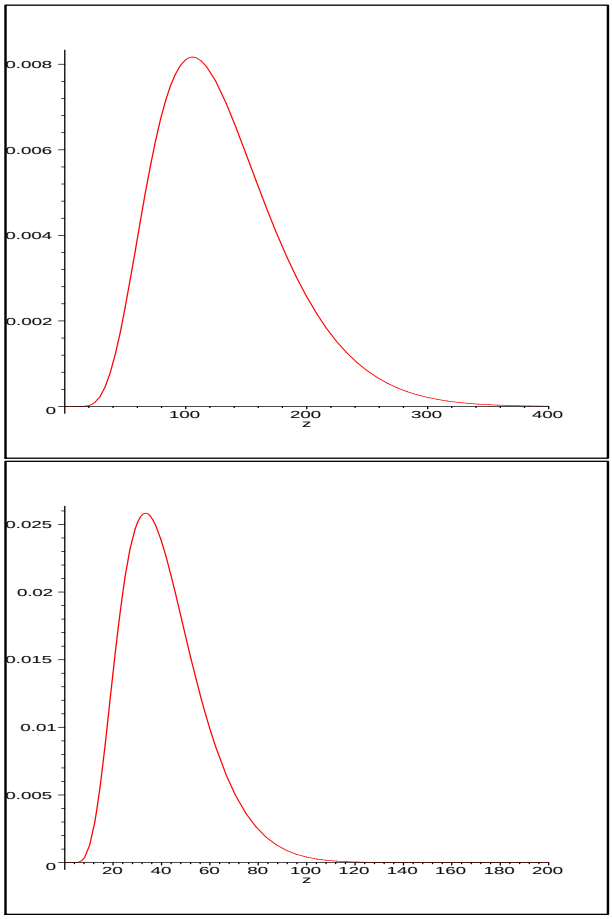

Figure 3: Stationary distributions (9) of $\mu_m = 0.01$ 1/s (top) and $\mu_m = 0.1$ 1/s (bottom) when $R_m = 0.1$ s.

In the RED case, the target buffer size b^* of the RED queue can then be obtained from the RED function $K(\cdot)$ (which prescribes the packet kill rate in function of buffer size) by solving the equation $K(b^*) = \beta$.

The assumption that RTTs do not fluctuate with time due to buffer content variations can easily be relaxed in this case by considering the more global fixed point problem (given here in the case where α_m is inversely proportional to the RTT of class m and where the discipline in the buffer of

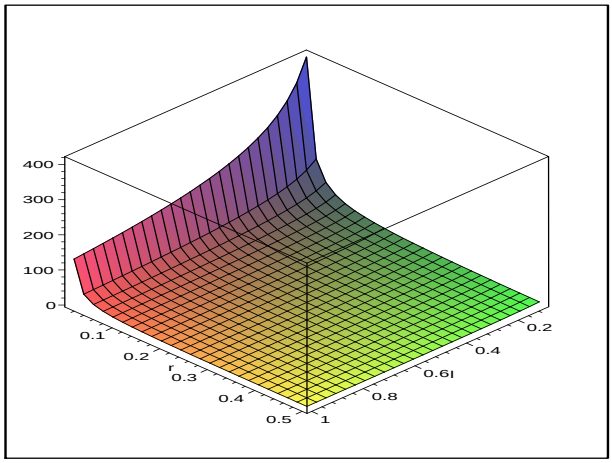

Figure 4: Mean of stationary distribution (10) over $\mu_m \in [0.02, 1]$ 1/s and $R_m \in [0.01, 0.5]$ s.

the shared link is FIFO):

$$\begin{aligned} \sum_m \frac{r_m}{d_m + b^*/c} \sqrt{\frac{2}{(\mu_m + \beta)}} &= c\sqrt{\pi} \frac{\prod_{k\geq 1}(1 - 2^{-2k+1})}{\prod_{k\geq 1}(1 - 2^{-2k})} \\ K(b^*) &= \beta, \end{aligned} \tag{15}$$

where $R_m = d_m + b^*/c$ with d_m the propagation delay and b^*/c the queuing delay.

Our analysis here is not limited to mean values. In both regimes, the stationary distribution of the rate obtained by each class can be derived using Formula (9). In the congestionless regime, (9) can be used directly. In the congestion regime, (9) should be used with μ_m replaced by $\mu_m + \beta$ for all m. The tail distribution of the stationary rate of a flow is of central importance within this context as it gives the proportion of time where the rate of this flow is above any given threshold, which can be seen as a weak form of QoS guarantee.

Example We illustrate the AQM case by the following scenario: there are two classes, a wireless-DSL class and a DSL class. The number $N_1 = N/2$ of wireless users is large and so is the number $N_2 = N/2$ of users of the DSL class. For class 1 (the wireless class) we take a rate dependent loss with $\mu_1 = 0.05$ 1/s, and a RTT $R_1 = 0.4$ s (resp. $\mu_1 = 0.03$ 1/s, and $R_1 = 0.3$ s). These figures are compatible with the measurements in [15]. For class 2 (the wired DSL class) we take $\mu_2 = 0.0001$ 1/s and $R_2 = 0.1$ s.

These two classes share a RED access link/router of capacity $c \times N$. If one takes $c = \infty$, one gets a congestionless regime where, according to (10), the mean value of class 1 is 14.64 (resp. 25.20) pkts/s. and that of class 2 is 1309.83 pkts/s. The load ρ is then $r_1\overline{x}^1 + r_2\overline{x}^2 = 662.235$ pkts/s. The ratio $\overline{x}^2/\overline{x}^1$ which measures the unfairness of the competition is in this case 89.47 (resp. 51.98).

If one now takes $c = 500$, the last formula allows one to find that the RED packet drop rate that stabilizes the system is $\beta = 0.000628$ (resp. $\beta = 0.000660$). Then the mean value of class 2 is 485.5 (resp. 475.13) pkts/s and that of class 1 is 14.5 (resp. 24.93) pkts/s. The unfairness ratio is now 33.5 (resp 19.06). In other words, class 2 is the only one to be really affected by bandwidth sharing.

4.2 The Tail-drop Case

For describing the congestion regime in the tail-drop case, we will need a more thorough analysis of the dynamics. We will use the following notation.

- T_n is n-th congestion time, namely the n-th epoch at which there are losses due to congestion on the shared router. It may even be the case where there are less than n congestion epochs (in which case we take $T_n = \infty$ by convention);
- $\tau_{n+1} = T_{n+1} - T_n$ whenever T_n is finite. By convention, we take $\tau_{n+1} = \infty$ whenever T_n is infinite;
- $X_n^i(t)$ is the throughput of flow i at time $T_n + t$ for $t \in [0, \tau_{n+1}]$ (we assume that all jump functions are right continuous);
- $X_n^m(t) = \dfrac{1}{N_m} \displaystyle\sum_{i=1}^{N_m} X_n^{i,m}(t)$;
- $\gamma_n^{(i)}$ is a $\{\frac{1}{2}, 1\}$-valued random variable with value $\frac{1}{2}$ if flow i experiences a loss at the n-th congestion time, 1 otherwise.

Here, the inter-congestion time τ_{n+1} is defined as

$$\inf \left\{ t > 0 \text{ s.t. } \sum_m \sum_i X_n^{i,m}(t) \; = \; C \right\}, \tag{16}$$

with $\tau_{n+1} = \infty$ if the last set is empty. The rationale for this definition stems from the assumption that the buffer capacity of the router is negligible (see the paper [11] for a simple way to relax this assumption), so that the next congestion takes place at the first time when the sum of all throughputs reaches again the capacity C of the router.

The mathematical derivations of this subsection focus on case with *rate independent synchronization*: the random variables $\{\gamma_n^{(i)}, i = 1, \ldots\}$ are independent of the past of the throughput processes just before the n-th congestion epoch and $\mathbb{P}(\gamma_n^{(i)} = \frac{1}{2}) = p$.

From this assumption, we have

$$\begin{aligned} \mathbb{E}[X_{n+1}^{i,m}(0)] &= \mathbb{E}\left[\gamma_{n+1}^{(i)}\right] \mathbb{E}\left[X_n^{i,m}(\tau_{n+1})\right] \\ &= \left(1 - \frac{p}{2}\right) \mathbb{E}\left[X_n^{i,m}(\tau_{n+1})\right]. \end{aligned}$$

So from (16), for all $n \geq 1$

$$\sum_m \sum_i \mathbb{E}[X_n^{i,m}(0)] \quad = \quad \left(1 - \frac{p}{2}\right) C.$$

Here we introduce a notation which will be used frequently throughout the paper:

$$c_n^m \quad = \quad \frac{1}{N_m} \sum_{i=1}^{N_m} \mathbb{E}[X_n^{i,m}(0)]. \tag{17}$$

Using the homogeneity assumption, we get that for all $n \geq 1$,

$$\sum_m r_m c_n^m \quad = \quad \left(1 - \frac{p}{2}\right) c. \tag{18}$$

When there exists a periodic congestion regime of period $\overline{\tau}$, we can write several useful invariance and cycle-mean equations.

The first general relation (19) expresses the periodicity of the rate at (just after) congestion epochs.

Let $S_m(z,t)$ be the solution of (4) (resp. (8) in the rate dependent case and (12) in the mixed case) with initial condition $S_m(z,0)$. The distribution of the rate of class m just after congestion $S_m(z,0)$ should satisfy the integral equation (which will be referred to as the invariant measure equation)

$$S_m(z,0) \quad = \quad (1-p) S_m(z,\overline{\tau}) \; + \; p S_m(2z,\overline{\tau}). \tag{19}$$

The solution $S_m(z,0)$ of this equation should then be used as the initial condition in (4) (resp. (8) and (12)) in order to express the stationary distribution of rates of class m in continuous time via the cycle-mean formula (see [16], Chapter 1):

$$S_m(z) \quad = \quad \frac{1}{\overline{\tau}} \int_{t=0}^{\overline{\tau}} S_m(z,t)\, dt. \tag{20}$$

In particular, the stationary, continuous time, mean value of the throughput of a flow of class m, which we will denote by $\overline{x}^m$ in what follows, can be calculated by the formula :

$$\overline{x}^m \quad = \quad \frac{1}{\overline{\tau}} \int_0^{\overline{\tau}} \int_0^{\infty} z\, S_m(z,t)\, dt\, dz. \tag{21}$$

4.2.1 Existence of a Congestion Regime in the RI Case

From (3) and (17), for the rate independent transmission-error case, the mean value (3) of a flow of class m of the congestion regime in the time interval $0 \leq t < \overline{\tau}_{n+1}$ is given by

$$\overline{X}_n^m(t) \quad = \quad (c_n^m - \overline{v}_m)\, e^{-\frac{\lambda_m}{2} t} \; + \; \overline{v}_m \tag{22}$$

with $\overline{v}_m$ in (6), and similarly the large population model (1) of the congestion regime is given by

$$\overline{X}_n(t) \quad = \quad \sum_m r_m \overline{X}_n^m(t). \tag{23}$$

We now address the following two natural questions: when do we have finite inter-congestion times ? What is the structure of the congestion regime (23) (e.g., fixed, periodic or chaotic) ?

First, we investigate the finiteness of the inter-congestion times. Let us define the load factor as

$$\rho \quad = \quad \sum_m r_m \overline{v}_m. \tag{24}$$

The next two lemmas show that the existence of infinitely many congestions is directly linked to the sign of $\delta = \rho - c$.

Lemma 6 *If $\rho > c$, the inter-congestion times $\overline{\tau}_{n+1}$ are finite for all $n \geq 0$. In addition, for all n*

$$\sum_m r_m \left(\overline{v}_m - c_n^m\right) e^{-\frac{\lambda_m}{2}\overline{\tau}_{n+1}} \quad = \quad \rho \; - \; c, \tag{25}$$

where

$$c_n^m \quad = \quad (c_0^m - \overline{v}_m)\left(1 - \frac{p}{2}\right)^n e^{-\frac{\lambda_m}{2}\sum_{k=1}^{n}\overline{\tau}_k} \; + \; \overline{v}_m \left(1 - \frac{p}{2}\right)\left(1 - \frac{p}{2}\Delta_n^m\right), \tag{26}$$

with $\Delta_n^m = \sum_{j=2}^{n} \left(1 - \frac{p}{2}\right)^{n-j} e^{-\frac{\lambda_m}{2}\sum_{k=j}^{n}\overline{\tau}_k}$ *and* $\Delta_1^m = 0$.

Proof: From (23), it is easy to see that if $\rho > c$, there is a finite t satisfying $\overline{X}_n(t) = c$ since $\overline{X}_n(t)$ is a continuous function and $\lim_{t\to\infty} \overline{X}_n(t) = \rho > c$ for any $n \geq 0$. Equations (25) and (26) are obtained by induction from (17), (22) and (23) when assuming finite congestion-times. ■

Lemma 7 *If $\rho \leq c$, $\overline{\tau}_{n+1} = \infty$ for some finite $n \geq 0$.*

Proof: Assume that $\overline{\tau}_{n+1}$ is finite for all n. Then from (26), for all $n \geq 1$,

$$c_n^m \quad \leq \quad (c_0^m - \overline{v}_m)\left(1 - \frac{p}{2}\right)^n e^{-\frac{\lambda_m}{2}\sum_{k=1}^{n}\overline{\tau}_k} \; + \; \overline{v}_m \left(1 - \frac{p}{2}\right).$$

Therefore, it is easy to see that $c_n^m < \overline{v}_m$ for all $n \geq n^*$, for some finite n^*, independently of c_0^m. From this fact and (23), we have $\sup_{t\geq 0} \overline{X}_n(t) < c$ for any $n \geq n^*$. ■

The physical interpretation of these results is that in the limiting system, it is only if random losses occur rarely enough that congestion plays a role in the regulation. The surprising fact is that the condition under which regulation involves congestion is very simple.

Next, we characterize the transient congestion regime (23).

Theorem 1 *If $\rho > c$, (23) admits a unique 1-periodic regime with period $\overline{\tau}$ satisfying*

$$\sum_m r_m c^m \quad = \quad c\left(1-\frac{p}{2}\right), \tag{27}$$

where c^m is given by

$$c^m \quad = \quad \begin{cases} \frac{\overline{v}_m\left(1-e^{-\frac{\lambda_m}{2}\overline{\tau}}\right)\left(1-\frac{p}{2}\right)}{\left(1-\left(1-\frac{p}{2}\right)e^{-\frac{\lambda_m}{2}\overline{\tau}}\right)} & \text{if } \lambda_m > 0 \\ 2\frac{\alpha_m}{R_m}\frac{\overline{\tau}}{p}\left(1-\frac{p}{2}\right) & \text{if } \lambda_m = 0 \end{cases} \tag{28}$$

with $\overline{v}_m$ in (6).

By 1-periodic, we maen that the period has exactly one intercongestion. The proof is given in Appendix 9.4. Equations (27) and (28) have no explicit solution in general but can be seen as a handy fixed point equation for determining $\overline{\tau}$ and c^m numerically.

The next corollary focuses on a special case where the period of the system $\overline{\tau}$ can be explicitly computed.

Corollary 1 *When all classes have the same $\lambda_m = \lambda > 0$, the inter-congestion times $\overline{\tau}_{n+1}$ are finite for all $n \geq 0$ iff $\rho > c$.*

In case $\rho > c$, the value of $\overline{\tau}_{n+1}$ is given by

$$\begin{aligned} \overline{\tau}_1 \quad &= \quad \frac{2}{\lambda}\log_e\left(1 \; + \; \frac{(c-\sum_m r_m c_0^m)}{\rho - c}\right) \\ \overline{\tau}_{n+1} \quad &= \quad \frac{2}{\lambda}\log_e\left(1 \; + \; \frac{pc}{2(\rho-c)}\right), \quad n \geq 1. \end{aligned} \tag{29}$$

In particular, if $\rho > c$, $\overline{\tau}$ is given by the last expression in (29).

Proof: The case with $\rho > c$ is shown in Lemma 6. Thus we have only to prove that if $\rho \leq c$, there is no finite inter-congestion time. When $\lambda_m = \lambda$ for all m except some classes with $\lambda_m = \infty$, (1) gives

$$\overline{X}_n(t) \quad = \quad \left(c\left(1-\frac{p}{2}\right) \; - \; \rho\right)e^{-\frac{\lambda}{2}t} \; + \; \rho. \tag{30}$$

From this equation, it is easy to see that either $\sup_{t\geq 0}\overline{X}_n(t) = X_n(0) = c\left(1-\frac{p}{2}\right)$ or $\overline{X}_n(t)$ is strictly increasing and tends to ρ for any $n \geq 0$. Thus there is no congestion if $\rho \leq c$. Equation (29) can easily be obtained from (30) with $\overline{X}_n(\overline{\tau}_{n+1}) = c$. ■

Three remarks are in order:

- When $\lambda_m = 0$ (which implies that $\rho > c$), (22) and (26) are replaced, respectively, by

$$\overline{X}_n^m(t) = c_n^m + \frac{\alpha_m}{R_m} t \tag{31}$$

$$c_n^m = c_0^m \left(1 - \frac{p}{2}\right)^n + \frac{\alpha_m}{R_m} \left(1 - \frac{p}{2}\right) \Delta_n^m \tag{32}$$

with $\Delta_n^m = \sum_{j=1}^{n} \left(1 - \frac{p}{2}\right)^{n-j} \overline{\tau}_j$. From (31), for all $n \geq 1$

$$\lim_{\forall \lambda_m \to 0} \overline{X}_n(t) = \sum_m r_m \frac{\alpha_m}{R_m} t + c\left(1 - \frac{p}{2}\right)$$

$$\lim_{\forall \lambda_m \to 0} \overline{\tau}_{n+1} = \frac{cp}{2 \sum_m r_m \frac{\alpha_m}{R_m}}. \tag{33}$$

- Notice that for each t, $\overline{X}_n(t)$ is a continuous function of $\lambda_m \in [0, \infty]$, and that (33) is the smallest possible inter-congestion time. Hence

$$\overline{\tau}_{n+1} \geq \frac{cp}{2 \sum_m r_m \frac{\alpha_m}{R_m}},$$

  for all $\lambda_m \geq 0$ and $n \geq 1$. Similarly, $\overline{X}_\infty(t)$ and $\overline{\tau}$ are continuous functions of $\lambda_m \in [0, \infty]$.

- For all $n \geq 1$, $\lim_{\lambda_m \to \infty} \overline{X}_n^m(t) = 0$.

We show below that the transient solution of the model with two classes converges to the unique $\overline{\tau}$-periodic limiting regime (27).

Theorem 2 *If $\rho > c$, the large population dynamic model for $m = 1, 2$ has unique $\overline{\tau}$-periodic limiting regime with*

$$\lim_{n \to \infty} \overline{\tau}_{n+1} = \overline{\tau} \quad \textit{and} \quad \lim_{n \to \infty} c_n^m = c^m. \tag{34}$$

The proof is given in Appendix 9.5. Simulation results based on *Netscale* [6] suggest that this result holds true for more than two classes, and also that there are no other stationary states than 1-periodic regimes.

4.2.2 Mean Values in the Congestion Regime of the RI Case

We first analyze the mean value of the $\overline{\tau}$-periodic limiting regime (27). Note that (21) can be rewritten as

$$\overline{x}^m = \frac{1}{\overline{\tau}} \int_0^{\overline{\tau}} \overline{X}_\infty^m(t)\, dt.$$

From (27) and (28), we obtain:

Corollary 2 *In the $\overline{\tau}$-periodic congestion regime, the mean value $\overline{x}^m$ of the throughput of a flow of class m is given by*

$$\overline{x}^m = \overline{v}_m - \frac{p\,\overline{v}_m}{\lambda_m \overline{\tau}} \frac{\left(1 - e^{-\frac{\lambda_m}{2}\overline{\tau}}\right)}{\left(1 - \left(1 - \frac{p}{2}\right) e^{-\frac{\lambda_m}{2}\overline{\tau}}\right)}. \tag{35}$$

Here are a few immediate consequences of this:

- We have the following continuity result:

$$\lim_{\lambda_m \to 0} \overline{x}^m = \frac{\alpha_m}{R_m}\overline{\tau}\left(\frac{2}{p} - \frac{1}{2}\right) = \overline{x}^m|_{\lambda_m = 0}. \tag{36}$$

- The stationary aggregated throughput ($\overline{x} \equiv \sum_m r_m \overline{x}^m$) is given by:
  - If $\lambda_m = 0$ for all m, $\overline{x} = c\left(1 - \frac{p}{4}\right)$;
  - If there are some classes with $\lambda_j = 0$,

$$\overline{x} = \sum_{i,\ \lambda_i > 0} r_i \left\{ \overline{v}_i + \frac{2}{\lambda_i \overline{\tau}} \left(c^i - \overline{v}_i\right) \left(1 - e^{-\frac{\lambda_i}{2}\overline{\tau}}\right) \right\} + \sum_{j,\ \lambda_j = 0} r_j \left(c^j + \frac{\alpha_j}{R_j} \frac{\overline{\tau}}{2} \right);$$

  - If $\rho > c$ and $\lambda_m > 0$ for all m,

$$\overline{x} = \rho - \frac{p}{\overline{\tau}} \sum_m r_m \frac{\overline{v}_m}{\lambda_m} \frac{\left(1 - e^{-\frac{\lambda_m}{2}\overline{\tau}}\right)}{\left(1 - \left(1 - \frac{p}{2}\right) e^{-\frac{\lambda_m}{2}\overline{\tau}}\right)};$$

  - If $\rho > c$ and $\lambda_m = \lambda$ for all m,

$$\overline{x} = \rho - \frac{cp}{2\log_e\left(1 + \frac{pc}{2(\rho - c)}\right)};$$

  - If there is no congestion ($\rho \leq c$),

$$\overline{x} = \rho. \tag{37}$$

We now analyze the sensitivity of the average throughput $\overline{x}$ and of other functions of interest with respect to the parameters of the model.

Theorem 3 *If $\rho > c$, we have*

$$c\left(1 - \frac{p}{4}\right) \leq \overline{x} < c. \tag{38}$$

The lower bound $c\left(1 - \frac{p}{4}\right)$ is only reached when $\lambda_m = 0$ for all m. The upper bound is only reached for $\rho = c$.

The proof is given in Appendix 9.6.

Corollary 3 *If $\rho > c$, for all m,*

$$\frac{d\overline{\tau}}{d\lambda_m} > 0 \quad \textit{and} \quad \frac{d\overline{x}^m}{d\lambda_k} > 0 \ \textit{for} \ \forall\, k \neq m. \tag{39}$$

The proof is given in Appendix 9.7.

It is easy to see that for all λ_m satisfying $\rho \leq c$, we have $\frac{d\overline{x}^m}{d\lambda_m} < 0$, $\frac{d\overline{x}^m}{d\lambda_k} = 0$ for $\forall\ m \neq k$ and $\frac{d\overline{x}}{d\lambda_m} < 0$ since then there is no interaction between classes. When $\rho > c$, unfortunately, it is very difficult to evaluate $\frac{d\overline{x}^m}{d\lambda_m}$ and $\frac{d\overline{x}}{d\lambda_m}$ except in a special case studied in the following corollary. However, we can easily see from Theorem 3 that there must be some range of λ_m satisfying $\frac{d\overline{x}}{d\lambda_m} > 0$ since $\overline{x}$ is a continuous function of each λ_m. This phenomenon is clear for the following special case.

Corollary 4 *In the case when $\lambda_m = \lambda$ for all m, $\overline{x}$ is an increasing function of ρ for $\rho \in [0, c]$ and a decreasing function of ρ for $\rho \in (c, \infty]$. Thus $\overline{x}$ achieves its maximal value c at $\rho = c$.*

Corollary 4 can be reinterpreted as follows: in the case when $\lambda_m = \lambda$ for all m, $\overline{x}$ is an increasing function of $\lambda \in \left[0,\ \sum_m r_m \frac{2}{c}\frac{\alpha_m}{R_m}\right]$, and a decreasing function of $\lambda \in \left[\sum_m r_m \frac{2}{c}\frac{\alpha_m}{R_m},\ \infty\right]$. Thus $\overline{x}$ achieves its maximal value "c" at $\lambda = \sum_m r_m \frac{2}{c}\frac{\alpha_m}{R_m}$.

In fact, Corollary 4 can be considered as an extension of [5] which studied the particular case $\lambda_m = \lambda$, $R_m = R$ and $\alpha_m = \alpha$ for all m, where the threshold in [5] was $\lambda^* = \frac{2}{c}\frac{\alpha}{R}$. Its proof follows that of Theorem 2 in [5].

4.2.3 Distributions in the Congestion Regime of the RI Case

The linear algebra procedures for the analysis of distributions will be introduced in §5.2.

Figure 5 and 6 give the solutions of the invariant measure equation (19) and of the stationary distribution in continuous time (20), respectively for competing wired and wireless classes. Notice the interesting fractal structure of the distribution of class 2. These curves were obtained independently by two different methods: numerical solutions based on *Mathcad* and simulations based on *Netscale* (see § 5).

4.2.4 The RD Transmission Error Case

We again define the load factor as

$$\rho \ = \ \sum_m r_m \overline{v}_m, \tag{40}$$

where $\overline{v}_m$ is the stationary mean value given by (10) of the free process defined in Lemma 4. By the same arguments as for Lemma 6, one gets:

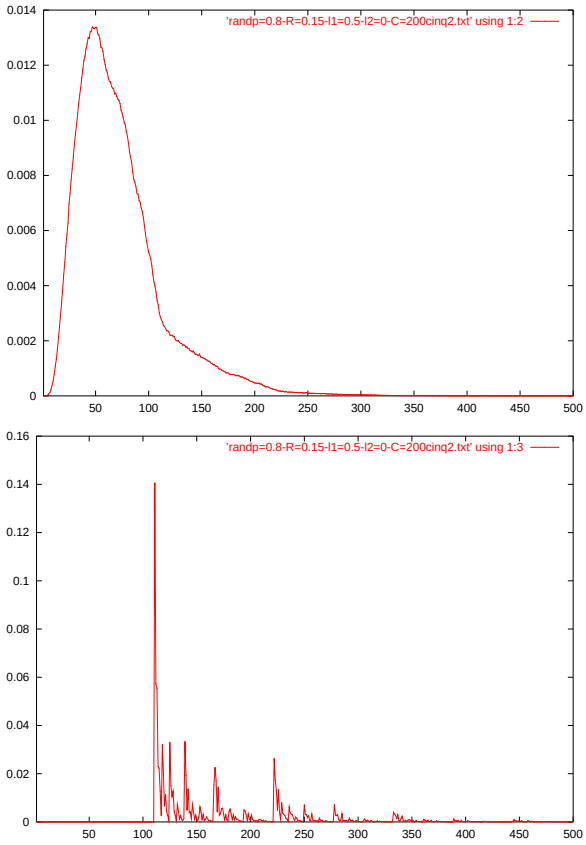

Figure 5: Distributions just after congestion (19) of classes with $\lambda_1 = 0.5$ 1/s (top) and $\lambda_2 = 0$ 1/s (bottom) when $p = 0.8$, $R_1 = R_2 = 0.15$ s., $c = 200$ pkts/s.

Lemma 8 *If $\rho > c$, the inter-congestion times $\overline{\tau}_{n+1}$ are finite for all $n \geq 0$.*

In the rate independent case, we had the closed form expression (3) for the mean value of the solution of (2). This was instrumental in the derivation of the closed form expression for the fixed point equation (27) satisfied by $\overline{\tau}$.

In the rate dependent case, such a closed form is unfortunately not available and we use in place a (linear algebra) numerical scheme similar to that presented in § 5.2.

Let the congestion regime be $\overline{\tau}$-periodic and $S_m^{<0>}$ be the solution of (19) for the RD case, which can be rewritten as a linear equation of the same shape as (47) (though with different matrices taking into account the RD dynamics). For all $\overline{\tau}$, one solves this linear equation using the same type of

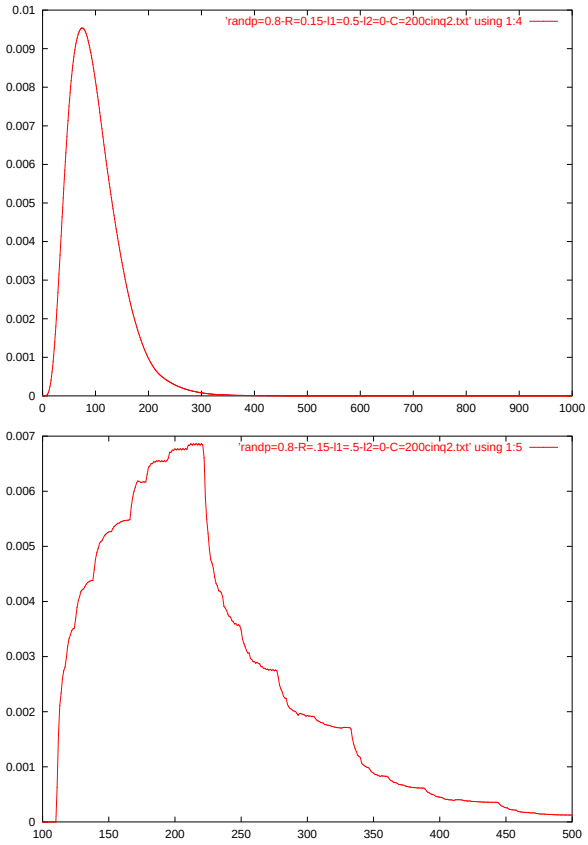

Figure 6: Distributions in continuous time (20) of classes with $\lambda_1 = 0.5$ 1/s (top) and $\lambda_2 = 0$ 1/s (bottom) when $p = 0.8$, $R_1 = R_2 = 0.15$ s., $c = 200$ pkts/s.

numerical scheme as in §5.2 to determine $S_m^{<0>}$ and then the stationary distribution of the rates for each class using the cycle-mean formula (20).

Here are two examples of fixed point equations allowing one to determine $\overline{\tau}$. In view of (18), $\overline{\tau}$ should be such that

$$\sum_m r_m \int_0^\infty z\, S_m(z,0)\, dz \quad = \quad \left(1 - \frac{p}{2}\right) c. \tag{41}$$

In all cases analyzed, this was sufficient to determine $\overline{\tau}$. Similarly, the total rate of increase of all flows should be matched by the total rate of decrease of all flows, so that this constant should be

such that

$$\sum_m r_m \frac{\alpha_m}{R_m} = \frac{pc}{2\overline{\tau}} + \sum_m r_m \frac{\mu_m}{2\overline{\tau}} \int_0^{\overline{\tau}} \int_0^{\infty} z^2 S_m(z,t) dz dt. \quad (42)$$

Figure 7 and 8, obtained independently by *Netscale* simulation and by the *Mathcad* numerical solver, illustrate the solutions of the invariant measure equation (19) and of the stationary distribution in continuous time (20), respectively, for two competing rate-dependent classes. The value of $\overline{\tau}$ in this case is 1.57 s. The average throughput $\overline{x}^m$ of each flow is 35.1 pkts/s for class 1 and 286.2 pkts/s for class 2.

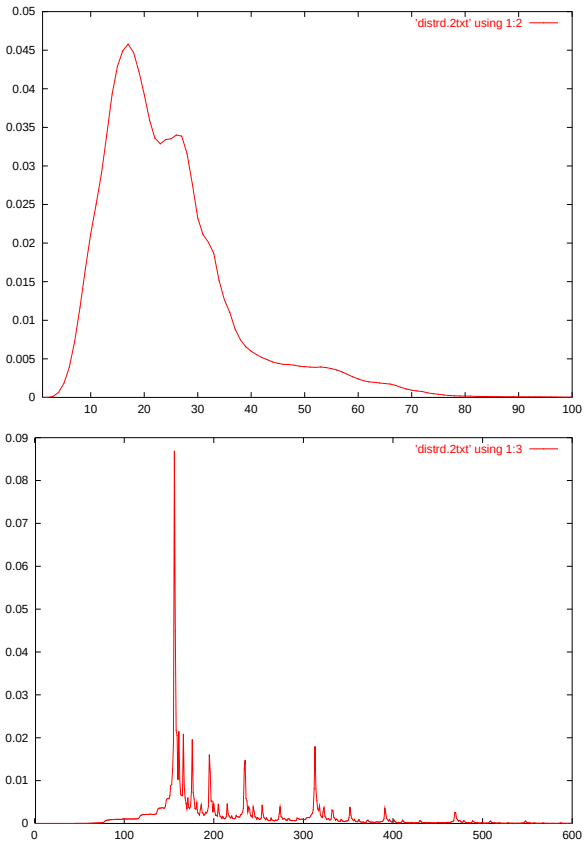

Figure 7: Distributions just after congestion (19) of rate-dependent classes with $\mu_1 = 0.02$ 1/s (top) and $\mu_2 = 0.00018$ 1/s (bottom) when $p = 0.8$, $R_1 = R_2 = 0.15$ s, $c = 200$ pkts/s.

The remaining question in the RD case is to find a necessary condition as in Lemma 7 and to prove the existence of a unique periodic limiting regime as in Theorem 1. Since we have no

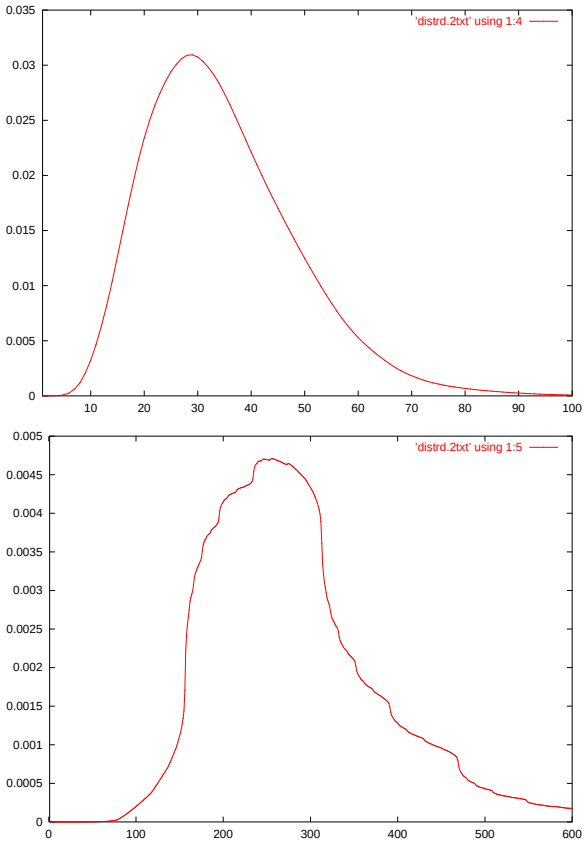

Figure 8: Distributions in continuous time (20) of rate-dependent classes with $\mu_1 = 0.02$ 1/s (top) and $\mu_2 = 0.00018$ 1/s (bottom) when $p = 0.8$, $R_1 = R_2 = 0.15$ s, $c = 200$ pkts/s.

mathematical way of addressing this question at the moment of the writing of this paper, we investigated numerically the conditions that drive the system in either the congestion or the congestionless regime. We found experimentally that as in the RI case, for all $\rho < c$, the only possible regime is congestionless.

4.2.5 The Mixed RI and RD Transmission Error Case

We use the same approach as in §4.2.4. In the mixed case, (42) is replaced by

$$\sum_m r_m \frac{\alpha_m}{R_m} \quad = \quad \frac{pc}{2\overline{\tau}} \; + \; \sum_m r_m \frac{1}{2\overline{\tau}} \int_0^{\overline{\tau}} \int_0^{\infty} (\lambda + \mu_m z) z \; S_m(z,t) \; dz dt. \tag{43}$$

This case is illustrated in §6.1.

5 Solution Methods

5.1 Formal Methods

All closed form solutions given in §3 are amenable to efficient *Maple* manipulation in spite of the fact that these formulas involve infinite products and series.

Let us illustrate this by a study of a DSL network with AQM or wireless networks experiencing rate-dependent transmission-error losses. There is often a tradeoff between the transmission error rate and RTT since it requires an additional processing time to reduce the transmission loss. One can use the stationary mean throughput (10) as a way to evaluate this tradeoff.

Figure 9 illustrates the use of Maple to study (10) on four types of tradeoffs between λ_m and RTT: $\lambda_m = l^{1.95}$ and $R_m = 0.1 + 1/\lambda_m$; $\lambda_m = l$ and $R_m = 0.1 + 1/\lambda_m$; $\lambda_m = l$ and $R_m = 0.1 - l/11$; and $\lambda_m = l$ and $R_m = 0.1 - l/25$ for $l = [0.01, 1]$. As shown in (10) and this figure, the relationship between the mean throughput and the transmission loss rate depends on the type of tradeoff between λ_m and RTT.

5.2 Numerical Methods

The Fredholm equations of §3 can be seen as linear systems when discretized. We give here a few hints on the discretization method used in the *Mathcad* code developed for this set of problems.

Given a certain value for the inter-congestion time $\overline{\tau}$, a numerical approximation of the distributions $s_m(z,t)\ \forall t \in [0, \overline{\tau}]$, $z \geq 0$ can be calculated with the following method.

We first sample the distributions and collect the samples in a matrix column vectors $S^{<j>}$:

$$S_m^{<j>}[i] \quad = \quad s_m\left((i+0.5)\frac{\Delta}{R^2}, j\Delta\right), \tag{44}$$

$i = 0, 1, \ldots, KL-1, \ \ j = 0, 1, \ldots, L$, with $\Delta = \frac{\overline{\tau}}{L}$. The parameter L controls the density of the sampling grid, while the parameter K determines the support (over z). Increasing these parameters improves the approximation, but the computational complexity as well ($L = 50$ and $K = 6$ are typical values used in this paper). Remark that $S_m^{<0>}$ and $S_m^{<L>}$ denote approximations of the distributions just after and just before a congestion epoch, respectively.

In this numerical framework, the Fredholm equations reduce to L linear equations:

$$S_m^{<j>} \quad = \quad \sum_{k=0}^{j-1} A_{m,k} S_m^{<k>} \ + \ B_m S_m^{<0>}, \ \ j = 1, 2, \ldots, L. \tag{45}$$

Solving these equations recursively yields a linear relation between the approximation of the distribution just after and just before a congestion epoch:

$$S_m^{<L>} \quad = \quad M S_m^{<0>}. \tag{46}$$

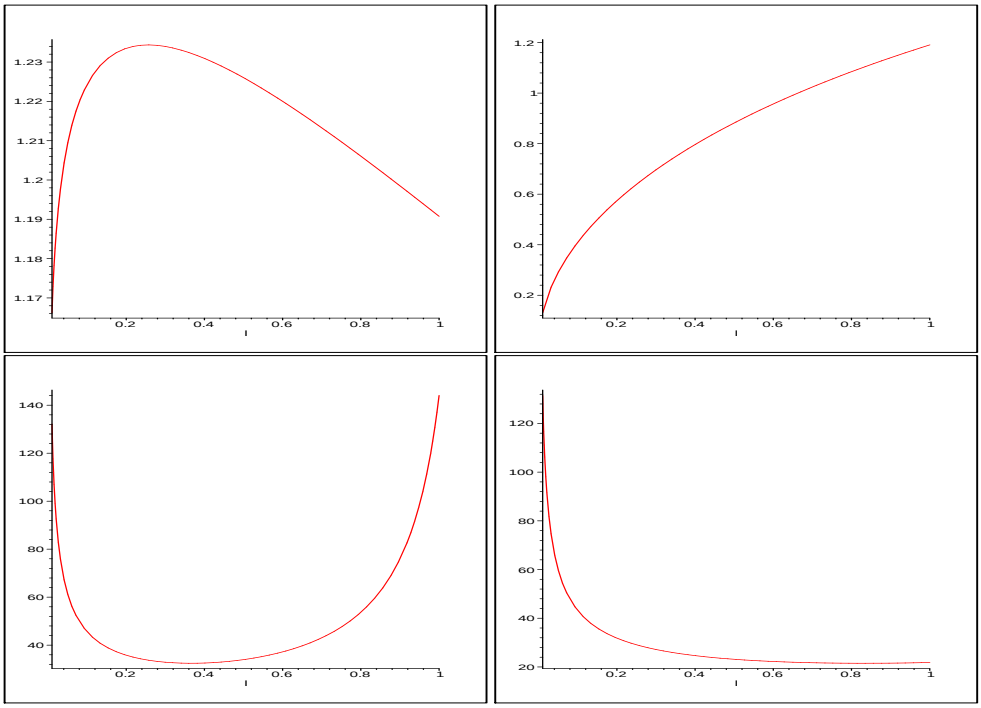

Figure 9: Mean of stationary distribution (10) depending on λ_m and R_m

The discretized version of the invariant measure equation (19) provides another relation between these two approximations for these distributions, i.e.,

$$S_m^{<0>} = PS_m^{<L>}. \tag{47}$$

Hence, $S_m^{<0>}$ can be found as the eigenvector associated to the eigenvalue 1 of the matrix PM, suitably scaled to obey the normalization constraint.

As the matrix M is not known explicitly, but calculated recursively, we find the eigenvector of PM by starting from an initial guess for $S_m^{<0>}$ and plugging it into the linear transformation described by (45) and (47) a sufficient amount of (typically 20) times. Convergence to a stable $S_m^{<0>}$ is rather quick.

5.3 Simulation of Large Population Models

For simulating large populations of TCP users, we use the flow level simulation approach described in [17] which is the basis of *Netscale* [6].

The typical setting used here is that with a single link shared by 10^5 flows of each class, which is a good compromise between the simulation time constraints and the quality of the approximation of the infinite population model by a finite population setting.

Below, we illustrate Theorem 2 and Theorem 3 using *Netscale*.

Figure 10 illustrates that the large population dynamic model (23) of competing wired and wireless TCP flows reaches the $\overline{\tau}$-periodic limiting regime after only a few congestion epochs. The average throughput $\overline{x} = \frac{1}{2}\overline{x}^1 + \frac{1}{2}\overline{x}^2$ of the limiting regime is around $\overline{x} = 161$ pkts/s which also illustrates (38), i.e.,

$$c\left(1 - \frac{p}{4}\right) = 160\, pkts/s \;\leq\; \overline{x} \;<\; c = 200\, pkts/s.$$

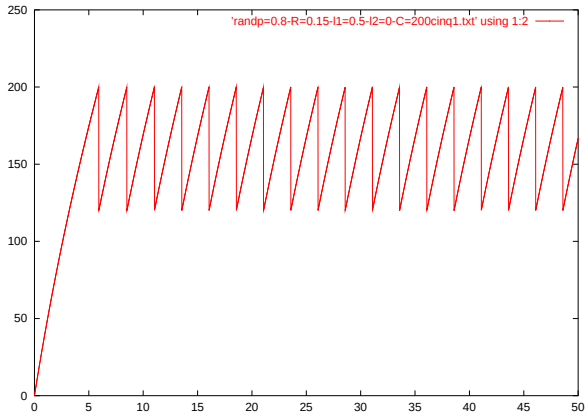

Figure 10: Throughput behavior of the large population dynamic model (23) when $p = 0.8$, $R_1 = R_2 = 0.15$ s., $\lambda_1 = 0.5$ 1/s, $\lambda_2 = 0$ 1/s and $c = 200$ pkts/s.

Figure 11 shows the dynamic behaviors of the wired and wireless large population dynamic models. As expected, the wired TCP flow with $\lambda_2 = 0$ 1/s has a larger average throughput than the wireless TCP flow with $\lambda_1 = 0.5$ 1/s when they have the same RTT.

6 Case Studies

6.1 Competition between Interleaved and Fast DSL Users

In DSL access [10], users can download files from the Internet over the copper pair which was traditionally used for telephony. The maximal downstream (i.e., in the direction from the network to the user) link rate that can be configured in Asymmetric DSL (ADSL) is 8 Mb/s (with a typical bit rate of 3 Mb/s being deployed in the field today). If we assume a packet size of 1500 bytes,

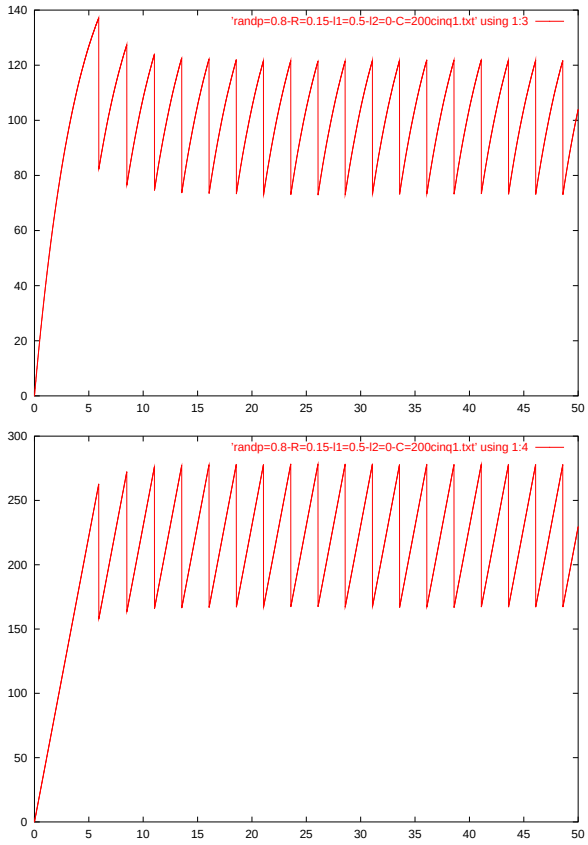

Figure 11: Throughputs (22) and (31) of classes with $\lambda_1 = 0.5$ 1/s (top) and with $\lambda_2 = 0$ 1/s (bottom) when $p = 0.8$, $R_1 = R_2 = 0.15$ s and $c = 200$ pkts/s.

this maximal link rate corresponds to 666.66 pkts/s. That is, of course, the maximal bit rate which each user can get. We suppose that in the network, the traffic of all users connected to this access network is aggregated in one aggregation node, where they compete for the available resources. In this bottleneck link, a capacity of $c = 200$ pkts/s per user is foreseen. We also assume that the link rate of 666.66 pkts/s does not influence the performance of TCP, and that the maximum window size of each flow is large enough not to choke the flow itself. So, as throughout the paper, we assume that the TCP performance is only affected by the congestion losses in the aggregation node and by the transmission errors on the DSL link.

The DSL access provider can configure a user's access link in two modes, referred to as *Fast* and *Interleaved*.

Table 1: Inter-congestion time and average rates for R =0.1 s

λ_1 [1/s]	$\overline{\tau}$ [s]	$\overline{x}^1$ [pkts/s]	$\overline{x}^2$ [pkts/s]
0	1.15	205.27	115.93
0.05	1.19	201.11	119.94
0.5	1.6	162.53	160.51
1	2.02	123.83	201.42

Table 2: Inter-congestion time and average rates for R =0.2 s

λ_1 [1/s]	$\overline{\tau}$ [s]	$\overline{x}^1$ [pkts/s]	$\overline{x}^2$ [pkts/s]
0	4.15	181.08	139.82
0.05	4.62	166.81	154.81
0.5	7.84	76.34	250.01
1	9.09	43.80	283.06

In *Fast* the bit transport is not heavily protected, so only 4 ms (2 ms in each direction) is added to the RTT. There are two types of loss events in this mode. First, Gaussian noise causes bit errors with an average rate of 1 bit error in 10^8 bits. Since each bit error leads to a packet loss, with the chosen packet size, this error event has the rate-dependent loss rate $\mu_m \approx 1.2 \times 10^{-4}$ 1/s. Second, there are packet losses due to impulsive noise on the line which has a rate-independent loss rate λ_m. Thus the error model of *Fast* corresponds to the mixed rate-independent/dependent transmission error case.

In *Interleaved*, the transport of the bits is protected by an interleaving and a forward error correction scheme against impulsive noise. Therefore, Gaussian noise is the only error source which affects performance: on average there is short burst of bit errors in 3×10^8 bits. Under these circumstances its rate-dependent loss rate is $\mu_m \approx 4 \times 10^{-5}$ 1/s. The penalty to pay for such a link less prone to errors is that the RTT increases up to about 40 ms (20 ms in each direction).

We now compare the impact of two modes on the TCP performance by the following scenario: *Fast* users are identified as class 1 whereas *Interleaved* users are identified as class 2; we set $N_1 = N_2$, $p = 0.8$, $c = 200$ pkts/s, $\mu_1 = 1.2 \times 10^{-4}$ 1/s, $\mu_2 = 4 \times 10^{-5}$ 1/s and $\lambda_2 = 0$ 1/s (i.e., there is no effect of impulsive noise in *Interleaved*); there are two sources contributing to RTT: the network outside the DSL introduces either $R = 0.1$ s or $R = 0.2$ s to RTT, hence, $R_1 = R + 0.004$ s and $R_2 = R + 0.04$ s. For the impulsive noise we consider four values λ_1 =0, 0.05, 0.5 and 1 1/s.

$\overline{\tau}$ and $\overline{x}^m$ in (21) for $m = 1,\ 2$ are calculated using the methodology described in §4.2.4. The results are displayed in Table 1 and 2. These tables illustrate that *Fast* achieves a higher throughput, if there is no impulsive noise. As the impulsive noise (i.e., λ_1) increases, the performance of *Interleaved* becomes better. The cross-over point, i.e., the value of λ_1 where both modes have the same average throughput depends on the contribution of R to RTT by the rest of the network: the higher R, the lower this cross-over point is.

6.2 Competition between Wireless and Wired Users

Consider the scenario in §4.1: competing wireless-DSL class and DSL class where $\mu_1 = 0.05$ 1/s, $R_1 = 0.4$ s, $\mu_2 = 0.0001$ and $R_2 = 0.1$ s.

If one now takes $c = 500$ pkts/s and a synchronization rate of $p = 0.8$, one finds a period of appr. 6.26 s and mean values of appr. 13.41 pkts/s for class 1 and of 784.56 pkts/s for class 2. The ratio $\overline{x}^2/\overline{x}^1$ is now 58.51. The degradation due to congestion affects much more the DSL class than the wireless class, where the ratio was 89.47 for the congestionless regime.

We keep the value of c fixed and equal to 500 pkts/s but we let now the packet loss rate μ_2 of the DSL class vary. In Figure 12, we observe a counter-intuitive phenomenon as discussed after Corollary 3: below a threshold (which is approximately the value of μ_2 for which the load ρ in the congestionless regime is equal to c), increasing μ_2 improves the average rates of both classes. Above this threshold, the rate of class 1 remains constant whereas that of class 2 degrades rapidly.

7 The Finite Population Model and Models based on Other Classes of Point Processes

Here, we come back to the general framework of §2.1. In particular, here, N and hence N_m are finite. The point processes are general (i.e. not necessarily Poisson). In addition, the probability that a given flow experiences a loss at a congestion epoch depends on the actual value of the throughput of this flow at this congestion epoch.

Let $\mathcal{L}^{i,m}$ denote the point process of the transmission error losses of flow i of class m. We assume that the point processes $\mathcal{L}^{i,m}$, $i = 1, \ldots, N_m$, $m = 1, \ldots, M$, are jointly stationary (see [16]). We assume that for fixed m, all point processes $\mathcal{L}^{i,m}$ have the same law (homogeneity assumption) and the same finite intensity λ_m. We denote by E_m the Palm probability of $\mathcal{L}^{i,m}$ (this probability does not depend on i by homogeneity).

In what follows, we assume that the dynamics of §2.1 admits a stationary regime and more precisely that the point process $\mathcal{C}$ of congestion epochs is jointly stationary with the point processes $\mathcal{L}^{i,m}$, $i = 1, \ldots, N_m$, $m = 1, \ldots, M$. We denote by E_C the Palm probability of $\mathcal{C}$ whenever this point process has a positive and finite intensity.

We denote

- by $X^m(t)$ the stationary throughput of one of the flows of class m at time t;
- by $\gamma(y)$ the random variable with value 1 if a flow of throughput y just before some congestion epoch experiences no loss and with value 1/2 otherwise;
- and by τ the intercongestion time $T_1 - T_0$.

The rate conservation principle (RCP), which applies to all discontinuous stationary processes (see [16], Chapter 1), states that the continuous algebraic growth rate of the process should compensate the algebraic growth of the process at jump times.

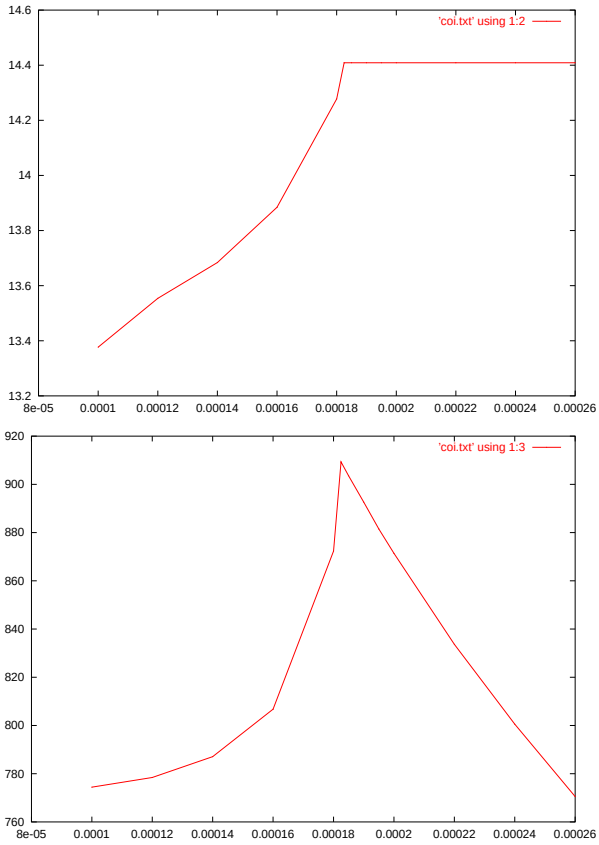

Figure 12: A small increase of the DSL loss rate improves performance. Average throughput $\overline{x}^1$ (top) and $\overline{x}^2$ (bottom) in function of μ_2 (see (21)).

Assume that the point process $\mathcal{C}$ has a finite intensity $\overline{\tau}^{-1} = E_C[\tau]^{-1}$. When applying the RCP to the discontinuous stationary process $X^m(t)$, this gives the following general conservation law:

$$\lambda_m \frac{E_m[X^m(0-)]}{2} + \frac{1}{\overline{\tau}}\left(E_C[X^m(0-)] - E_C[X^m(0-)\gamma(X^m(0-))]\right) = \frac{\alpha_m}{R_m}. \quad (48)$$

In the case when there are no congestion points at all, then

$$E_m[X^m(0-)] = \frac{2\alpha_m}{\lambda_m R_m} = \overline{v}_m. \quad (49)$$

In the particular case when the loss point processes are RI-Poisson, we know that there are infinitely many congestion epochs when N_m is finite. In this case, the PASTA property implies that

$E_m[X^m(0-)] = \overline{x}^m$, so that we then have

$$\overline{x}^m \;=\; \overline{v}_m \;-\; \frac{2\Big(E_C[X^m(0-)] - E_C[X^m(0-)\gamma(X^m(0-))]\Big)}{\lambda_m \overline{\tau}}.$$

If in addition synchronization is rate independent, then

$$\overline{x}^m \;=\; \overline{v}_m \;-\; \frac{E_C[X^m(0-)]p}{\lambda_m \overline{\tau}}.$$

This equation holds for all finite N_m. However, for finite N_m, all of $\overline{x}^m$, $E_C[X^m(0-)]$ and $E_C[\tau]$ are unknown. Notice that for $N_m = \infty$, the above equation is compatible with (35).

We now return to the general framework of the beginning of this section.

Lemma 9 *If $\rho > c$ and if the underlying point processes are ergodic, there is a.s. an infinite number of congestion epochs.*

Proof: The proof is by contradiction. If there are no congestion points at all, then (49) holds. Since largest possible value of $\sum_m r_m \overline{v}_m \;=\; \rho$ is c, we then have $\rho \leq c$. ■

8 Conclusions

The competition between several classes of TCP flows for an access link/router leads to complex nonlinear dynamical systems with an evolution represented by integral and partial differential equations. The analysis of these systems leads to closed form formulas for the throughput obtained by each class in the simplest cases and leads to efficient linear algebraic numerical methods in most cases.

In the presence of bit/packet error rates for all classes, two regimes are possible: a congestionless regime where the regulation is made by the random transmission losses, and a congestion regime where packet losses/discards in the shared link/router are necessary to control the flows. The conditions that drive the competing flows in one of these two regimes are in terms simple threshold conditions on the load brought by these flows.

Several general physical phenomena are identified:

- in the tail-drop case, for loads above the threshold that separates these regimes, a small increase of the bit/packet error rate of any flow improves performance for *all* flows and leads to a better utilization of the link;
- the unfairness of the competition between flows with small and large bit/packet error rates is less pronounced in the congestion regime than in the congestionless regime.

It is also shown that this approach allows one to analyze specific scenarios typical of current access networks, with a mix of wired, DSL and wireless users and in particular to compare the merits of coding schemes that propose different tradeoffs between bit/packet error rate and latency.

9 Appendix

9.1 Proof of Lemma 1, 3, 5

Here we prove Lemma 5, where Lemma 1 and Lemma 3 are special cases of Lemma 5. We define the Laplace transform

$$\widehat{s}_m(z,u) \quad = \quad \int_0^\infty e^{-ut} s_m(z,t)dt. \tag{50}$$

Taking the Laplace of (11) w.r.t. t, we get

$$u\widehat{s}_m(z,u) \; - \; s_m(z,0) \; + \; \frac{\alpha_m}{R_m}\frac{\partial}{\partial z}\widehat{s}_m(z,u) \; = \\ \lambda_m(2\widehat{s}_m(2z,u) - \widehat{s}_m(z,u)) \; + \; \mu_m z(4\widehat{s}_m(2z,u) - \widehat{s}_m(z,u))$$

or equivalently

$$\frac{\partial}{\partial z}\widehat{s}_m(z,u) \quad = \quad -\frac{R_m}{\alpha_m}(u+\lambda_m+\mu_m z)\widehat{s}_m(z,u) \; + \; \frac{R_m}{\alpha_m}(s_m(z,0) + (2\lambda_m + 4\mu_m z)\widehat{s}_m(2z,u)).$$

The solution of this ODE is

$$\widehat{s}_m(z,u) \quad = \quad \frac{R_m}{\alpha_m}\int_0^z e^{-\frac{R_m}{\alpha_m}\left((u+\lambda_m)(z-x)+\frac{\mu_m}{2}(z^2-x^2)\right)}\left(s_m(x,0) + (2\lambda_m + 4\mu_m x)\widehat{s}_m(2x,u)\right)dx.$$

The solution (12) is obtained by direct Laplace inversion of the last expression.

9.2 Proof of Lemma 2

The density $\sigma_m(z)$ satisfies the equation

$$\frac{\alpha_m}{R_m}\frac{d\sigma_m}{dz}(z) \quad = \quad \lambda_m(2\sigma_m(2z) - \sigma_m(z)). \tag{51}$$

Let $\widehat{\sigma}_m(u)$ be the Mellin transform of $\sigma_m(z)$:

$$\widehat{\sigma}_m(u) \quad = \quad \int_0^\infty \sigma_m(z) z^{u-1} dz \tag{52}$$

with $u \geq 1$. Multiplying both sides of the last equation by z^u and integrating w.r.t. z, we get

$$u\widehat{\sigma}_m(u) \quad = \quad \lambda_m \frac{R_m}{\alpha_m}\widehat{\sigma}_m(u+1)\left(1-2^{-u}\right).$$

Let

$$\widehat{\sigma}_m(u) \quad = \quad f_m(u)\Gamma(u)\left(\frac{\alpha_m}{\lambda_m R_m}\right)^u.$$

Then from the fact that $\Gamma(u+1) = u\Gamma(u)$, we have $f_m(u) = f_m(u+1)(1-2^{-u})$, that is

$$f_m(u) \quad = \quad \phi \prod_{k\geq 0}(1-2^{-u-k}),$$

where ϕ is a constant. So

$$\widehat{\sigma}_m(u) \quad = \quad \phi\Gamma(u)\left(\frac{\alpha_m}{\lambda_m R_m}\right)^u \prod_{k\geq 0}(1-2^{-u-k}).$$

Since $\widehat{\sigma}_m(1) = 1$ and $\Gamma(1) = 1$, we get the expression for ϕ. Using now the relation

$$\int_0^\infty e^{-at}t^{u-1}dt \quad = \quad a^{-u}\Gamma(u)$$

we obtain that

$$\sigma_m(t) \quad = \quad \phi \sum_{n\geq 0} a_n e^{-\left(\lambda_m \frac{R_m}{\alpha_m} 2^n\right)t}.$$

9.3 Proof of Lemma 4

The proof procedure is similar to that of Appendix 9.2. The density $\sigma_m(z)$ satisfies the equation

$$\frac{\alpha_m}{R_m}\frac{d\sigma_m}{dz}(z) \quad = \quad \mu_m(4z\sigma_m(2z) - z\sigma_m(z)). \tag{53}$$

Multiplying both sides of the last equation by z^{u-1} and integrating w.r.t. z, we get

$$\frac{\alpha_m}{R_m}(u-1)\widehat{\sigma}_m(u-1) \quad = \quad \mu_m\widehat{\sigma}_m(u+1)\left(1-2^{-u+1}\right)$$

or equivalently

$$\frac{\alpha_m}{R_m}u\widehat{\sigma}_m(u) \quad = \quad \mu_m\widehat{\sigma}_m(u+2)\left(1-2^{-u}\right).$$

Let

$$\widehat{\sigma}_m(u) \quad = \quad f_m(u)\Gamma\left(\frac{u}{2}\right)\left(\frac{2\alpha_m}{\mu_m R_m}\right)^{\frac{u}{2}}.$$

Then $f_m(u) = f_m(u+2)(1-2^{-u})$, that is

$$f_m(u) \quad = \quad \phi \prod_{k\geq 0}(1-2^{-u-2k}),$$

where ϕ is a constant. So

$$\widehat{\sigma}_m(u) \quad = \quad \phi\Gamma\left(\frac{u}{2}\right)\left(\frac{2\alpha_m}{\mu_m R_m}\right)^{\frac{u}{2}} \prod_{k\geq 0}(1-2^{-u-2k}).$$

Since $\Gamma\left(\frac{1}{2}\right) = \sqrt{\pi}$, we get the expression for ϕ. Using now the relation

$$2\int_0^\infty e^{-av^2} v^{u-1} dv \;=\; \int_0^\infty e^{-at} t^{\frac{u}{2}-1} dt \;=\; a^{-\frac{u}{2}}\Gamma\left(\frac{u}{2}\right)$$

we obtain that

$$\sigma_m(t) \;=\; 2\phi \sum_{n\geq 0} a_n e^{-\left(\frac{\mu_m R_m}{2\alpha_m} 4^n\right)t^2}.$$

9.4 Proof of Theorem 1

From (17) and (22), with $c_n^m = c^m$ and $\overline{\tau}_{n+1} = \overline{\tau}$ we have

$$c^m \;=\; \begin{cases} \left(\left(c^m - \overline{v}_m\right) e^{-\frac{\lambda_m}{2}\overline{\tau}} + \overline{v}_m\right)\left(1 - \frac{p}{2}\right) & \text{if } \lambda_m > 0 \\ \left(c^m + \frac{\alpha_m}{R_m}\overline{\tau}\right)\left(1 - \frac{p}{2}\right) & \text{if } \lambda_m = 0. \end{cases} \tag{54}$$

Thus we can see that there exists a positive solution $\overline{\tau}$

$$\overline{\tau} \;=\; \begin{cases} \frac{2}{\lambda_m}\log_e\left(\frac{\left(1-\frac{p}{2}\right)}{1+\frac{p}{2}\frac{\overline{v}_m}{\left(c^m-\overline{v}_m\right)}}\right) & \text{if } \lambda_m > 0 \\ c^m \frac{R_m}{\alpha_m}\frac{p}{(2-p)} & \text{if } \lambda_m = 0 \end{cases} \tag{55}$$

if $0 < c^m < \overline{v}_m\left(1 - \frac{p}{2}\right)$ for all m ($c^m = \overline{v}_m = 0$ when $\lambda_m = \infty$). This condition requires that $\sum_m r_m c^m = c\left(1 - \frac{p}{2}\right) < \sum_m r_m \overline{v}_m \left(1 - \frac{p}{2}\right) = \rho\left(1 - \frac{p}{2}\right)$ which is satisfied with $\rho > c$. Next, we check uniqueness of such $\overline{\tau}$ and c^m when $0 < c^m < \overline{v}_m\left(1 - \frac{p}{2}\right)$ and $\rho > c$. First, we consider the case where $\lambda_m > 0$ for all m. If we put (54) into (27), the resulting equation can be rewritten as

$$\sum_m r_m \left(\overline{v}_m - c^m\right) e^{-\frac{\lambda_m}{2}\overline{\tau}} \;=\; \rho \;-\; c.$$

In the above equation, the left side can be rewritten as

$$\frac{p}{2}\sum_m \frac{r_m \overline{v}_m e^{-\frac{\lambda_m}{2}\overline{\tau}}}{\left(1 - \left(1 - \frac{p}{2}\right)e^{-\frac{\lambda_m}{2}\overline{\tau}}\right)}$$

that is a monotonically decreasing function of $\overline{\tau}$ with a value in $(0, \rho - c\left(1 - \frac{p}{2}\right))$, so the above equation has a unique positive solution when $\rho > c$.

In the case where there are several classes with $\lambda_i > 0$ and $\lambda_j = 0$, uniqueness can be proved using

$$\sum_i r_i \left(\overline{v}_i - c^i\right) e^{-\frac{\lambda_i}{2}\overline{\tau}} \;-\; \sum_j r_j \left(c^j + \frac{\alpha_j}{R_j}\overline{\tau}\right) \;=\; \sum_i r_i \overline{v}_i \;-\; c.$$

9.5 Proof of Theorem 2

The key step for proving convergence of the large population dynamic behavior for all $m = 1, 2$ is to introduce the definition

$$e_n \quad = \quad r_1 \left(c_n^1 - c^1\right) \quad = \quad r_2 \left(c^2 - c_n^2\right), \tag{56}$$

noting that $r_1 c_n^1 + r_2 c_n^2 = r_1 c^1 + r_2 c^2 = c(1 - \frac{p}{2})$ for all $n \geq 1$. First, we consider the case where $\lambda_m > 0$ for all m. The case where either $\lambda_1 = 0$ or $\lambda_2 = 0$ will be discussed in the end of this proof. Theorem 1 and (56) allow us to characterize the model (1) as follows.

Lemma 10 *If $\rho > c$, for each $n \geq 1$*

1. $\overline{\tau}_{n+1} > \overline{\tau}$ *iff* $e_n > 0$ *when* $\lambda_1 > \lambda_2$;
2. $\overline{\tau}_{n+1} > \overline{\tau}$ *iff* $e_n < 0$ *when* $\lambda_1 < \lambda_2$;
3. $\overline{\tau}_{n+1} = \overline{\tau}$ *iff* $e_n = 0$ *when* $\lambda_1 \neq \lambda_2$;
4. $\overline{\tau}_{n+1} < \overline{\tau}$ *iff* $e_n < 0$ *when* $\lambda_1 > \lambda_2$;
5. $\overline{\tau}_{n+1} < \overline{\tau}$ *iff* $e_n > 0$ *when* $\lambda_1 < \lambda_2$.

When $\lambda_1 = \lambda_2$, $\overline{\tau}_{n+1}$ is given by (29) regardlessly of e_n.

Proof: From (22),

$$c_{n+1}^m \quad = \quad \left((c_n^m - \overline{v}_m)\, e^{-\frac{\lambda_m}{2}\overline{\tau}_{n+1}} \; + \; \overline{v}_m\right)\left(1 - \frac{p}{2}\right). \tag{57}$$

From (54), (57) and $r_1 c_n^1 + r_2 c_n^2 = r_1 c^1 + r_2 c^2$, we know that

$$r_1 \left(\overline{v}_1 - c_n^1\right) e^{-\frac{\lambda_1}{2}\overline{\tau}_{n+1}} + r_2 \left(\overline{v}_2 - c_n^2\right) e^{-\frac{\lambda_2}{2}\overline{\tau}_{n+1}} \quad = \quad r_1 \left(\overline{v}_1 - c^1\right) e^{-\frac{\lambda_1}{2}\overline{\tau}} + r_2 \left(\overline{v}_2 - c^2\right) e^{-\frac{\lambda_2}{2}\overline{\tau}}.$$

From this equation and (56), we can get

$$\begin{aligned} e_n \quad = \quad & \frac{1}{\left(e^{-\frac{\lambda_2}{2}\overline{\tau}_{n+1}} - e^{-\frac{\lambda_1}{2}\overline{\tau}_{n+1}}\right)} \Bigg\{ r_1 \left(\overline{v}_1 - c^1\right)\left(e^{-\frac{\lambda_1}{2}\overline{\tau}} - e^{-\frac{\lambda_1}{2}\overline{\tau}_{n+1}}\right) \\ & + \; r_2 \left(\overline{v}_2 - c^2\right)\left(e^{-\frac{\lambda_2}{2}\overline{\tau}} - e^{-\frac{\lambda_2}{2}\overline{\tau}_{n+1}}\right) \Bigg\}. \end{aligned}$$

This concludes the proof. ■

Lemma 11 *If $\rho > c$, for any $i, j \geq 1$*

1. $e_i > 0$ *iff* $e_j > 0$;

2. $e_i = 0$ *iff* $e_j = 0$;

3. $e_i < 0$ *iff* $e_j < 0$.

Proof: From (54), (56) and (57),

$$e_{n+1} = \left(e_n e^{-\frac{\lambda_1}{2}\overline{\tau}_{n+1}} + r_1 \left(\overline{v}_1 - c^1\right) \left(e^{-\frac{\lambda_1}{2}\overline{\tau}} - e^{-\frac{\lambda_1}{2}\overline{\tau}_{n+1}} \right) \right) \left(1 - \frac{p}{2}\right) \quad (58)$$

$$= \left(e_n e^{-\frac{\lambda_2}{2}\overline{\tau}_{n+1}} + r_2 \left(\overline{v}_2 - c^2\right) \left(e^{-\frac{\lambda_2}{2}\overline{\tau}_{n+1}} - e^{-\frac{\lambda_2}{2}\overline{\tau}} \right) \right) \left(1 - \frac{p}{2}\right). \quad (59)$$

When $\lambda_1 = \lambda_2 > 0$, (58) and (59) are given by $e_{n+1} = e_n e^{-\frac{\lambda_1}{2}\overline{\tau}} \left(1 - \frac{p}{2}\right)$ since then $\overline{\tau}_{n+1} = \overline{\tau}$ for all $n \geq 1$. When $\lambda_1 \neq \lambda_2$, Lemma 10 completes the proof using (58) for $\lambda_1 > \lambda_2$ and (59) for $\lambda_1 < \lambda_2$. ■

Lemmas 10 and 11 directly lead to the following result.

Lemma 12 *If $\rho > c$, for any $i, j \geq 2$*

1. $\overline{\tau}_i > \overline{\tau}$ *iff* $\overline{\tau}_j > \overline{\tau}$;

2. $\overline{\tau}_i = \overline{\tau}$ *iff* $\overline{\tau}_j = \overline{\tau}$;

3. $\overline{\tau}_i < \overline{\tau}$ *iff* $\overline{\tau}_j < \overline{\tau}$.

Now, we are ready to study the limiting behavior of e_n which directly leads to Theorem 2.

Corollary 5 *If $\rho > c$,*

$$\lim_{n\to\infty} e_n = 0. \quad (60)$$

Proof: From Lemma 11, we have only to deal with the case $e_1 \neq 0$. From (58) and (59),

$$e_n = e_1 e^{-\frac{\lambda_1}{2}\sum_{j=2}^{n}\overline{\tau}_j} \left(1 - \frac{p}{2}\right)^{n-1} + r_1 \left(\overline{v}_1 - c^1\right) \sum_{j=2}^{n} \left(e^{-\frac{\lambda_1}{2}(\overline{\tau} - \overline{\tau}_j)} - 1 \right) e^{-\frac{\lambda_1}{2}\sum_{i=j}^{n}\overline{\tau}_i} \left(1 - \frac{p}{2}\right)^{n-j+1} \quad (61)$$

$$= e_1 e^{-\frac{\lambda_2}{2}\sum_{j=2}^{n}\overline{\tau}_j} \left(1 - \frac{p}{2}\right)^{n-1} + r_2 \left(\overline{v}_2 - c^2\right) \sum_{j=2}^{n} \left(1 - e^{-\frac{\lambda_2}{2}(\overline{\tau} - \overline{\tau}_j)} \right) e^{-\frac{\lambda_2}{2}\sum_{i=j}^{n}\overline{\tau}_i} \left(1 - \frac{p}{2}\right)^{n-j+1}. \quad (62)$$

In the case where $\overline{\tau}_{n+1} = \overline{\tau}$ for all $n \geq 1$, it is easy to see that $\lim_{n\to\infty} e_n = 0$ since the first terms in the right-hand sides of (61) and (62) go to zero as $n \to \infty$ regardlessly of e_1. In the case where $\overline{\tau}_{n+1} \neq \overline{\tau}$, the second terms in the right-hand sides of (61) and (62) have different signs as shown in Lemma 12. Thus $\lim_{n\to\infty} e_n = 0$. ■

All results in this section hold for the special case where either $\lambda_1 = 0$ or $\lambda_2 = 0$, which can be interpreted as the case where $\rho > c$. Next, we summarize the corresponding results for the case where $\lambda_1 > \lambda_2 = 0$ (the case that $\lambda_2 > \lambda_1 = 0$ can be studied symmetrically).

- $\overline{\tau}_{n+1} > \overline{\tau}$ iff $e_n > 0$, $\overline{\tau}_{n+1} = \overline{\tau}$ iff $e_n = 0$, and $\overline{\tau}_{n+1} < \overline{\tau}$ iff $e_n < 0$. This can be proved using

$$e_n = \frac{1}{\left(1 - e^{-\frac{\lambda_1}{2}\overline{\tau}_{n+1}}\right)} \left\{ r_1 \left(\overline{v}_1 - c^1\right) \left(e^{-\frac{\lambda_1}{2}\overline{\tau}} - e^{-\frac{\lambda_1}{2}\overline{\tau}_{n+1}} \right) + r_2 \frac{\alpha_2}{R_2} (\overline{\tau}_{n+1} - \overline{\tau}) \right\}$$

- The above two results directly lead to Lemmas 11, 12 and Corollary 5. Note that in this case, (59) and (62) are replaced, respectively, by

$$\begin{aligned} e_{n+1} &= \left(e_n + \frac{\alpha_2}{R_2} (\overline{\tau} - \overline{\tau}_{j+1}) \right) \left(1 - \frac{p}{2}\right) \\ e_n &= e_1 \left(1 - \frac{p}{2}\right)^{n-1} + \sum_{j=2}^{n} \frac{\alpha_2}{R_2} (\overline{\tau} - \overline{\tau}_j) \left(1 - \frac{p}{2}\right)^{n-j+1}. \end{aligned}$$

9.6 Proof of Theorem 3

It is easy to see that $\overline{x} < c$ since $\overline{\tau}$ is finite for all $\lambda_m \in [0, \infty]$.

Next, we prove the lower bound. First, we can easily see that $\overline{x} = c\left(1 - \frac{p}{4}\right)$ from (36) and the cycle mean formula, when $\rho > c$ and $\lambda_m = 0$ for all m except some classes with $\lambda_m = \infty$, where $c_n^m = 0$ for all $n \geq 1$ if $\lambda_m = \infty$. Second, we show that $\overline{x} > c\left(1 - \frac{p}{4}\right)$ if $\rho > c$ and $\lambda_i > 0$ for some i. In this case, from (22) and (28), we see that

$$\begin{aligned} \frac{d\overline{X}_\infty(t)}{dt} &= \sum_{i,\ \lambda_i > 0} r_i \frac{\lambda_i}{2} (\overline{v}_i - c^i) e^{-\frac{\lambda_i}{2}t} + \sum_{j,\ \lambda_j = 0} r_j \frac{\alpha_j}{R_j} > 0 \\ \frac{d^2\overline{X}_\infty(t)}{dt^2} &= -\sum_{i,\ \lambda_i > 0} r_i \left(\frac{\lambda_i}{2}\right)^2 (\overline{v}_i - c^i) e^{-\frac{\lambda_i}{2}t} < 0. \end{aligned}$$

Thus $\overline{X}_\infty(t)$ is a strictly increasing concave function of t. Therefore, using the fact that $\overline{X}_\infty(0) = c\left(1 - \frac{p}{2}\right)$ and $\overline{X}_\infty(\overline{\tau}) = c$, we have

$$\overline{x} = \frac{\int_0^{\overline{\tau}} \overline{X}_\infty(t)\, dt}{\overline{\tau}} > \frac{\overline{X}_\infty(0) + \overline{X}_\infty(\overline{\tau})}{2} = c\left(1 - \frac{p}{4}\right).$$

Finally, $\overline{x}$ has c at $\rho = c$ as shown in (37).

9.7 Proof of Corollary 3

Define

$$\begin{aligned} K_{\lambda_m} &= e^{-\frac{\lambda_m}{2}\overline{\tau}}, \qquad A_{\lambda_m} = \left(1-\left(1-\frac{p}{2}\right)K_{\lambda_m}\right) \\ B_{\lambda_m} &= \sum_m r_m \left(\frac{\alpha_m}{R_m}\right)\left(\frac{K_{\lambda_m}}{A^2_{\lambda_m}}\right)\left(\frac{p}{2}\right). \end{aligned} \tag{63}$$

Note that $K_{\lambda_m} \in [0,1]$ with $K_0 = 1$ and $K_\infty = 0$.

From (27), (35) and (36), for all $m \neq k$ we can derive

$$\begin{aligned} \frac{d\overline{\tau}}{d\lambda_m} &= \left(\frac{r_m \overline{v}_m}{\lambda_m A^2_{\lambda_m} B_{\lambda_m}}\right) f(K_{\lambda_m}) \\ \frac{d\overline{x}^m}{d\lambda_k} &= \begin{cases} \left(\frac{p\overline{v}_m}{\lambda_m A^2_{\lambda_m}\overline{\tau}^2}\right) f(K_{\lambda_m})\frac{d\overline{\tau}}{d\lambda_k} & \text{if } \lambda_m > 0 \\ \frac{\alpha_m}{R_m}\left(\frac{2}{p}-\frac{1}{2}\right)\frac{d\overline{\tau}}{d\lambda_k} & \text{if } \lambda_m = 0 \end{cases} \end{aligned}$$

with $f(K_{\lambda_m}) = A_{\lambda_m}(1-K_{\lambda_m}) + \frac{p}{2}K_{\lambda_m}\log_e K_{\lambda_m}$. Since $\frac{df(K_{\lambda_m})}{dK_{\lambda_m}} = 2\left(1-\frac{p}{2}\right)(K_{\lambda_m}-1) + \frac{p}{2}\log_e K_{\lambda_m} < 0$ for all $K_{\lambda_m} \in [0,1)$, $\frac{df(K_{\lambda_m})}{dK_{\lambda_m}}|_{K_{\lambda_m}=1} = 0$ and $f(1) = 0$, it is easy to see that $f(K_{\lambda_m}) > 0$ for all $K_{\lambda_m} \in [0,1)$. This concludes the proof.

References

[1] ITU-T (Telecommunication standardization sector of International Telecommunication Union), "Asymmetric digital subscriber line ADSL transceivers," in *Recommendation G.922.1*, June 1999.

[2] H. Balakrishnan, V. N. Padmanabhan, S. Seshan, and R. H. Katz, "A comparison of mechanisms for improving TCP performance over wireless links," *IEEE/ACM Transactions on Networking*, vol. 5, pp. 756–769, December 1997.

[3] C. Barakat, E. Altman, and W. Dabbous, "On TCP performance in a heterogeneous network: a survey," *IEEE Communications Magazine*, vol. 38, 2000.

[4] J. Liu, I. Matta, and M. Crovella, "End-to-end interface of loss nature in a hybrid wired/wireless environment," in *Proc. of the workshop (WiOpt'03)*, March 2003.

[5] F. Baccelli and K. B. Kim, "TCP throughput analysis under transmission error and congestion losses," in *Proc. of IEEE Infocom*, (Hong Kong), 2004.

[6] D. Hong, *N2NSOFT*. `http://www.n2nsoft.com/`, 2003.

[7] "ATM over ADSL recommendations," tech. rep., 1997. TR-002,`http://www.dslforum.org/aboutdsl/TR-002.doc`.

[8] E. N. Gilbert, "Capacity of a burst-noise channel," *Bell Syst. Tech. Journal*, vol. 39, pp. 1253–1265, 1960.

[9] H. Sanneck, G. Carle, and R. Koodli, "A framework model for packet loss metrics based on loss runlengths," in *SPIE/ACM SIGMM Multimedia Computing and Networking Conference*, January 2000.

[10] T. Starr, J. M. Cioffi, and P. J. Silverman, *Understanding Digital Subscriber Line Technology*. ISBN 0137805454, 1999.

[11] F. Baccelli and D. Hong, "AIMD, fairness and fractal scaling of TCP traffic," in *Proc. of IEEE Infocom*, April 2002.

[12] K. B. Kim and S. H. Low, "Analysis and design of AQM based on state-space models for stabilizing TCP," in *Proc. of IEEE American Control Conference*, (Denver, Colorado), pp. 260–265, 2003.

[13] K. B. Kim, "Design of feedback controls supporting TCP based on modern control theories," tech. rep., INRIA, Paris, France, 2003. RR 5014 (Submitted to IEEE Transactions on Automatic Control).

[14] F. Baccelli, D. R. McDonald, and J. Reynier, "A mean-field model for multiple TCP connections through a buffer implementing RED," *Performance Evaluation*, vol. 49, pp. 77–97, 2002.

[15] C. Hoene, A. Günther, and A. Wolisz, "Measuring the impact of slow user motion on packet loss and delay over IEEE 802.11b wireless links," in *Workshop on Workshop on Wireless Local Networks (WLN)*, October 2003.

[16] F. Baccelli and P. Brémaud, *Elements of Queueing Theory*. Springer Verlag, 1994.

[17] F. Baccelli and D. Hong, "Flow level simulation of large IP networks," in *Proc. of IEEE Infocom*, April 2003.

Unité de recherche INRIA Rocquencourt
Domaine de Voluceau - Rocquencourt - BP 105 - 78153 Le Chesnay Cedex (France)

Unité de recherche INRIA Lorraine : LORIA, Technopôle de Nancy-Brabois - Campus scientifi que
615, rue du Jardin Botanique - BP 101 - 54602 Villers-lès-Nancy Cedex (France)
Unité de recherche INRIA Rennes : IRISA, Campus universitaire de Beaulieu - 35042 Rennes Cedex (France)
Unité de recherche INRIA Rhône-Alpes : 655, avenue de l'Europe - 38330 Montbonnot-St-Martin (France)
Unité de recherche INRIA Sophia Antipolis : 2004, route des Lucioles - BP 93 - 06902 Sophia Antipolis Cedex (France)

Éditeur
INRIA - Domaine de Voluceau - Rocquencourt, BP 105 - 78153 Le Chesnay Cedex (France)
http://www.inria.fr
ISSN 0249-6399